Improved forest canopy evaporation leads to better predictions of ecohydrological processes

Henrique Haas, Latif Kalin, Haw Yen

ABSTRACT

Canopy evaporation (E_i) is a vital process in forest ecosystems impacting hydrology and biogeochemistry through the redistribution of gross rainfall and gradual infiltration of water into the soil profile. Inaccurate representation of E_i in models may lead to flawed predictions of ecohydrological processes such as water availability, soil erosion, nutrient transport, and ecosystem productivity, thus compromising the reliability of model outputs. The Soil and Water Assessment Tool (SWAT) ecohydrological model has been widely used for various purposes worldwide. However, SWAT has shown limitations in forest ecosystems. SWAT employs a single equation to calculate canopy evaporation for crops and trees, which may not accurately account for the differences in ecophysiology and aerodynamic resistance between short and tall vegetation. In SWAT, canopy interception is calculated as a function of canopy storage and is normalized by the maximum plant leaf area index (LAI). Here we present an alternative approach to simulate forest canopy interception and evaporation with SWAT. Under our proposed approach, the LAI normalization is eliminated, and canopy storage is computed as a linear function of daily LAI and a user-defined parameter. We used remote-sensing (R-S) estimates of E_i to accurately parameterize forest canopy evaporation in the modified and default models. The Alabama-Coosa-Tallapoosa, a large (55,000 km^2) and forested watershed system in the Southeast United States, is utilized as testbed. Results showed that the default SWAT largely underestimated (> 70%) forest E_i across our study domain. The modified model better matched R-S estimates of E_i, showing a mere 2% overestimation. Additionally, the modified model yielded better agreement with R-S transpiration and total evapotranspiration compared to the default model. Our alternative approach positively affected the model simulation of daily streamflow and ecologically relevant flow metrics, reducing model overestimations and leading to better agreement with observations. Also, the modified model led to reduced sediment, nitrate, and organic nitrogen loadings, with sediment and organic nitrogen being particularly affected, witnessing reductions of 13 and 11%, respectively, compared to the default model. Finally, our proposed approach resonated in better agreement between simulated net primary productivity (NPP) and R-S estimates. Although our study is in the context of SWAT, our findings can be useful to the broader modeling community since other popular process-based models are based on similar modeling assumptions. Our findings demonstrate the benefits of improved forest evapotranspiration partitioning for simulating ecological processes with SWAT.

KEYWORDS: Canopy evaporation, forest modelling, ecosystem services, SWAT, remote sensing

1. Introduction

Canopy rainfall interception is the process by which vegetation captures and temporarily stores gross rainfall (P) before it reaches the ground (Lawrence et al., 2007; Nicholls and Carey, 2021; Paul-Limoges et al., 2020; Stoy et al., 2019) - being the first of several land surface hydrological processes affecting the redistribution of rainwater (Brantley et al., 2019; Miralles et al., 2010). Canopy evaporation (E_i) represents a major fraction of the global terrestrial evapotranspiration (ET), making it a key, yet understudied, component of the terrestrial water and energy budgets (Hadiwijaya et al., 2021; Muzylo et al., 2009). This process is particularly relevant in forest ecosystems, where E_i usually represents 10 to 40% of the total ET (Brantley et al., 2019; Kofroňová et al., 2021; Miralles et al., 2010). Canopy interception and evaporation may also influence soil erosion and nutrient exports by facilitating the gradual infiltration of water into the soil profile and thereby minimizing the erosive power of rapid surface runoff (Zore et al., 2022). In forest ecosystems, the nexus between the soil-plant-atmosphere is stronger because of higher aerodynamic conductance associated with taller vegetation (Miralles et al., 2010; Muzylo et al., 2009). Thus, forest canopy interception is an important link between land surface and atmosphere influencing terrestrial biogeochemistry and water balance.

Different techniques (e.g., lysimeters, eddy covariance, leaf gas exchange, models) have been used to measure and estimate forest canopy interception and evaporation. Field studies are usually costly, labor-intensive, time-consuming, and not feasible for performing continuous measurements over large areas (Muzylo et al., 2009; Yu et al., 2022). Process-based numerical models have been increasingly used in environmental sciences and applied to estimate canopy interception and evaporation (Kofroňová et al., 2021; Wang et al., 2007; M. Yang et al., 2018). Examples are land surface models (LSM) (e.g., *Community Land Model (CLM)*), watershed models (e.g., *Soil and Water Assessment Tool (SWAT)*), and stand-scale models (e.g., *Physiological Processes Predicting Growth (3-PG)*).

The SWAT model (Arnold et al., 1998) has been widely used to predict ecological processes like water availability (Angela et al., 2015; Bekele et al., 2013; Venkatesh et al., 2020), soil erosion (dos Santos et al., 2023; Karakoyun and Kaya, 2022; Luo et al., 2023), nutrient transport (Grizzetti et al., 2003; Isik et al., 2023; Jiang et al., 2023), carbon sequestration (Bekele et al., 2013; Liang et al., 2022; Q. Yang et al., 2018), and plant growth (Nair et al., 2011; Strauch and Volk, 2013; Yang and Zhang, 2016). As of December 2023, there were over 5,300 peer-reviewed journal articles employing SWAT around the globe (https://www.card.iastate.edu/swat_articles/). Despite its popularity, previous studies have identified certain limitations of SWAT in forest ecosystems (Alemayehu et al., 2017; Haas et al., 2022a, 2022b; Strauch and Volk, 2013; Yang and Zhang, 2016). The default model parameters controlling tree growth and dynamics have primarily been derived from personal communication and generalized forest studies (Neitsch et al., 2011). Additionally, SWAT employs a single equation to calculate canopy evaporation for crops and trees, which may not accurately account for the differences in ecophysiology and aerodynamic resistance between short and tall vegetation.

Past studies have addressed SWAT's limitations in forest ecosystems by either improving its parameterization of forest processes and dynamics (Haas et al., 2021; Yang and Zhang, 2016) or by modifying the model's structure to enhance the representation of forest attributes such as leaf area index (LAI) (Alemayehu et al., 2017; Guo et al., 2018; Strauch and Volk, 2013). Other studies have modified the model's vegetation growth module (Karki et al., 2023; Lai et al., 2020) or assimilated remote-sensing information (e.g., ET, LAI) into the model (Rajib et al., 2018b, 2020). However, to the best of the author's knowledge, no study to date has assessed SWAT's skills in capturing canopy evaporation or presented alternatives to enhance this process. Additionally, studies involving severe modification of the model's source code may increase modeling complexity and require additional files and parameters, hindering their applicability to regular users.

Accurately representing forest E_i in SWAT can have important implications for modeling ecosystem services such as water availability, ecological flows, soil erosion control, nutrient transport, and plant growth. For instance, E_i directly impacts total ET in SWAT. In highly forested regions such as the southeast united states (SE-US), ET can be as high as 90% of the incoming rainfall (McLaughlin et al., 2013). Thus, E_i can have substantial impacts on ecosystem water balance. Furthermore, E_i impacts the amount of P reaching the ground in SWAT, which may influence the timing and rate of simulated streamflow (Neitsch et al., 2011). Indirectly, plant biomass in SWAT is influenced by E_i through the partitioning of transpiration, canopy evaporation, and soil evaporation. This, in turn, can impact soil erosion, given that the Universal Soil Loss Equation (USLE) (Williams, 1975) cover and management factor is calculated as a function of plant biomass in SWAT (Neitsch et al., 2011). Plant biomass and residue also play a role in nutrient uptake and residue mineralization in SWAT. Thus, improving the mechanistic representation of forest E_i might positively influence the modeling of ecohydrological processes (e.g., energy, water, nutrient cycling) and strengthen model results. Water is a key driver of ecological processes (Sun et al., 2017) and combining accurate ecohydrological predictions with ecosystem services (e.g., water quality purification, carbon sequestration, flood and drought attenuation) can be valuable in providing science-based outputs for policy and decision-making.

With the rise of open-access datasets (e.g., remote-sensing information) and open-source simulation tools, modelers are met with the possibility of enhancing the representation of ecohydrological processes once overlooked or ignored in numerical models. However, studies such as Komatsu and Kume (2020) highlight the necessity of using more practical models with simplified structures in forest hydrology to facilitate communications among stakeholders. The increased availability of remote-sensing (R-S) information may contribute to the simplification of ecological processes in numerical models through the development of empirical relationships. In recent years, several high-resolution and freely available products describing processes like net primary productivity (NPP), transpiration (E_t), canopy evaporation, and soil evaporation (E_s) have been developed (Robinson et al., 2018; Running and Zhao, 2019; Zhang et al., 2019). Additionally, the advent of cloud-based geospatial platforms such as Google Earth Engine (GEE) (Gorelick et al., 2017) has facilitated the acquisition and processing of large-scale remote sensing data and their application in Earth system sciences. Despite the availability of global estimates of ecological processes such as E_i and NPP, this information has not been sufficiently explored in ecohydrological modeling yet.

Considering SWAT's limitations in forest ecosystems and the lack of studies assessing its skills in predicting canopy evaporation, we modified the source code to introduce a new canopy interception equation specifically designed for forests. More specifically, we set out to answer the following research questions: (i) how accurately is E_i represented in SWAT? (ii) what is the significance of forest E_i for simulating ecohydrological processes such as water availability, ecological flows, sediment yield, nutrient transport, and ecosystem productivity? (iii) can improved E_i representation enhance streamflow simulation in SWAT? We test our methodology in the Alabama-Coosa-Tallapoosa (ACT) river basin, a large and forested watershed in Alabama-USA. Here we compare the results obtained with the modified model against those of the default SWAT. We hope to open new avenues in leveraging freely available datasets to enhance model predictability and ensure the robust application of ecohydrological models in forest ecosystems.

2. Methods and Data

2.1. The SWAT Model

The Soil and Water Assessment Tool (SWAT) (Arnold et al., 1998) is an ecohydrological model that can simulate several horizontal (e.g., surface runoff, lateral flow, groundwater contribution), and vertical (e.g., ET, E_t, E_i, E_s, percolation) water fluxes, as well as sediment loss, nutrient loadings, and plant growth. SWAT is equipped with plant growth and management modules that allow for the representation of different plant physiologies (e.g., evergreen, deciduous, and mixed forests) and silvicultural practices (planting, biomass harvesting, fertilization) in the model (Neitsch et al., 2011). The integrative nature of SWAT comprising water, climate, vegetation, soil, and management components provides a comprehensive framework for estimating outputs that can be interpreted as ecosystem services.

SWAT discretizes a watershed into subwatersheds, which are further discretized into unique combinations of land use, soils, and slope called hydrological response units (HRU's) (Neitsch et al., 2011). The water balance at the HRU level is calculated as:

$$\Delta S = \sum_{t=1}^{t}(P - Q_{total} - ET - w_{seep}) \quad (1)$$

where, ΔS is the change in water storage in the soil profile, P, Q_{total}, ET, and w_{seep} are the daily amount of precipitation, total water yield, evapotranspiration, and the total amount of water exiting the bottom of the soil profile on a given day, respectively. The total water yield (Q_{total}) is the sum of surface runoff, lateral flow, and base flow contributions to streamflow.

In the current study, surface runoff was computed using the NRCS-CN method based on daily rainfall observations, and the Muskingum method (Cunge, 1969) was used to route runoff volume from the subbasins to the main channel. The Penman-Monteith (P-M) (Monteith, 1965) method was selected for estimating potential evapotranspiration (PET).

The vegetation growth module of the SWAT model is based on a simplified version of the EPIC cropping system model (Williams, 1990) and uses the same set of equations to model canopy interception and evaporation from all types of plants. Total actual evapotranspiration (AET) is the sum of transpiration, canopy evaporation, and soil evaporation. Canopy evaporation is calculated from the amount of water intercepted by the vegetation canopy as a function of user-defined maximum canopy storage and maximum LAI:

$$can_{day} = can_{mx} \cdot \frac{LAI}{LAI_{mx}} \qquad (2)$$

where can_{day} is the maximum amount of water that can be held in the canopy on a given day (mm), can_{mx} is a user-defined maximum amount of water that can be trapped in the canopy when the canopy is fully developed (mm), LAI is the leaf area index on a given day and LAI_{mx} is a user-defined maximum leaf area index for the plant.

If P is smaller than can_{day} minus the initial amount of water held in the canopy (I_i) on a given day:

$$I_f = I_i + P \quad (3)$$

$$P_{net} = 0 \quad (4)$$

where I_f is the final amount of water held in the canopy (mm), and P_{net} is the amount of rainfall reaching the ground (mm).

If $P \geq can_{day} - I_i$

$$I_f = can_{day} \quad (5)$$

$$P_{net} = P - (can_{day} - I_i) \quad (6)$$

When calculating AET, SWAT first evaporates any rainfall intercepted by the plant canopy according to equations 7-10. If PET is smaller than the total amount of water held in the canopy (I) (mm):

$$AET = E_i = PET \quad (7)$$

$$I_f = I_i - E_i \quad (8)$$

On the other hand, if $PET > I$:

$$E_i = I \quad (9)$$

$$I_f = 0 \quad (10)$$

The remaining evaporative water demand is partitioned between the vegetation and the soil. When using the Penman-Monteith (P-M) PET method in SWAT, transpiration is approximated as the plant water uptake for the day and determined as a function of soil water content and a user-defined plant water uptake compensation coefficient. Soil evaporation in SWAT is calculated as a function of soil water content, aboveground biomass and residue, soil depth, and a user-defined soil evaporation compensation factor (Neitsch et al., 2011). Details regarding SWAT's computation of E_t and E_s are provided in the Supplementary Materials file.

2.2. An alternative forest canopy interception method

Here we introduce an alternative method to model canopy interception for forests in SWAT. Under our proposed approach, forest canopy storage is modeled as a function of LAI and a user-controlled parameter, according to equation 11:

$$S_{can} = c \, . \, LAI \quad (11)$$

where S_{can} is the amount of water stored in the canopy (mm), c is a user-defined parameter (mm), and LAI is the plant leaf area index for the day (m^2/m^2). This method was initially introduced by Leyton et al. (1967) and Rutter et al. (1971) and has since then been used in LSM such as the Canadian Land Surface Scheme (Verseghy et al., 1993). A similar approach is used in the CLM 4.5 (Oleson et al., 2013) LSM model. Studies such as Noilhan and Planton (1989) advocated for this approach as a simplistic, yet robust, method for representing forest canopy interception in general circulation models

(GCMs). Water balance studies at the plot and watershed scales have applied this method to estimate forest canopy interception and shown values of c ranging from 0.2 to 0.5 (Amatya et al., 1996; J. McCarthy et al., 1991; Spittlehouse and Black, 1981).

In the current study, the subroutines *canint.f*, *hruaa.f*, *hruday.f*, *hrumon.f*, *hruyr.f*, and *sumv.f* in the source code of SWAT 2012 Rev. 664 were modified to represent forest canopy interception according to Eq. 11. For other land-use classes not classified as forests in SWAT, canopy interception was modeled with the equations described in section 2.1.

The simulated values of canopy evaporation, transpiration, and soil evaporation are not printed in the default versions of SWAT. In the current study, we modified the model's source code to print these variables at the HRU level in the *output.hru* file. The values of canopy evaporation, transpiration, and soil evaporation are printed over the variables 36 (PGRZ), 37 (CFERTN), and 38 (CFERTP), respectively, as defined in the *.cio* file and described in the model's input/output documentation (Arnold et al., 2011).

2.3. Study area

The Alabama-Coosa-Tallapoosa (ACT) river basin (Figure 1) was selected to study the importance of accurately representing forest canopy evaporation in watershed models. The ACT river basin is a large (59,100 km^2) and mainly forested (61% forest cover) watershed that contributes over 50% of the water discharged to the Mobile Bay - a large estuary along the Gulf of Mexico coast with strategic economic and ecological importance for the state of Alabama (Coogan et al., 2019). According to the National Forest Types Dataset (Ruefenacht et al., 2008), the main evergreen forest (FRSE) species in the ACT river basin is loblolly pine (*Pinus taeda L.*), whilst white and red oaks are the dominant deciduous forest (FRSD) species (Figure S1 in the Supplementary material file). The basin drains large rivers such as the Coosa, Tallapoosa, Cahaba, and Alabama, and spans across Alabama, northwest Georgia, and southern Tennessee, making it a good testbed for investigating the importance of forest canopy evaporation in regional watershed modeling. The ACT river basin is home to a diverse range of flora and fauna, including many rare and endangered aquatic species (Deutsch, 2019). The watershed also plays an important role in drinking water supply, agriculture, and industry throughout the region (Atkins et al., 2004). Average elevation ranges from near sea level to 1,280 meters according to the 30-meter resolution National Elevation Dataset (NED) (NED, 1999). The annual average precipitation and temperature are 1,400 mm and 17 °C, respectively, characterizing the watershed as warm and humid. In terms of soil distribution, sandy loam, and silty loam soils are predominant across the watershed area (Soil Survey Geographic Database (SSURGO)).

For this study, five watersheds ranging from 4,572 km^2 (Cahaba river watershed) to 55,615 km^2 (Alabama river watershed) within the ACT river basin and with varying physical characteristics (e.g., annual rainfall, average temperature, discharge, elevation, and forest cover) (Table 1), were selected to assess the effects of forest canopy evaporation on the model predictions of ecological processes at different scales and under various environmental conditions.

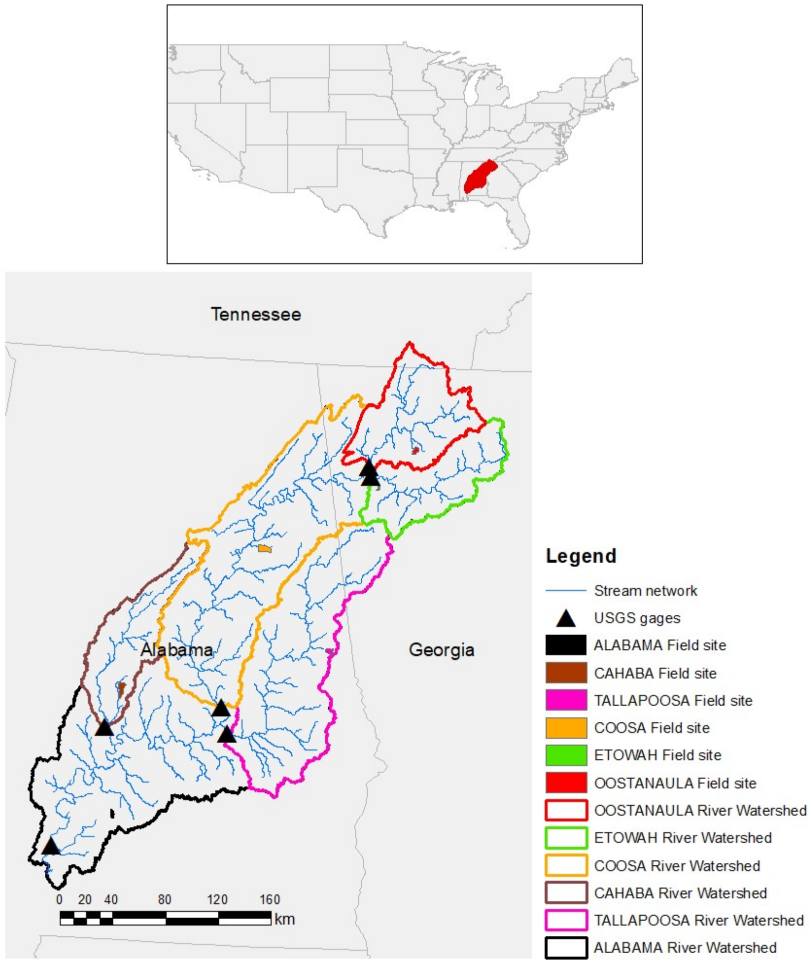

Figure 1 – The study area showing the entire Alabama-Coosa-Tallapoosa river basin, along with five smaller watershed systems, and the selected field-scale sites where forest canopy evaporation was calibrated to capture the basin's heterogeneities.

Table 1 – Physical characteristics of the study watersheds. The average values of rainfall, temperature, and streamflow are from the period 1980-2020. Average forest cover comprises the average of evergreen (FRSE), deciduous (FRSD), and mixed (FRST) forests within each watershed.

	Drainage area (km^2)	**Annual rainfall (mm)**	**Average daily air temperature (°C)**	**Average annual streamflow (mm)**	**Mean elevation (m)**	**Dominant physiographic region**	**% of FRSE cover**	**Average % of Forest cover**
Cahaba	4,572	1448	17.4	520	141	Coastal Plain	24	61
Alabama	55,615	1374	16.9	432	199	Coastal Plain	21	69
Tallapoosa	12,066	1371	17.1	411	221	Piedmont	24	62
Coosa	26,175	1368	16.2	504	269	Valley and Ridge	17	63
Oostanaula	5,481	1334	15.4	562	345	Valley and Ridge	13	65
Etowah	4,666	1298	14.4	506	335	Piedmont	13	62

2.4.Model setup and input data

The ArcSWAT 2012 (version 10.4.19) ArcMap interface was used in this study to delineate the ACT river basin, discretize it into subbasins and tributaries, and create the HRUs. Watershed delineation was carried out from a 10-meter resolution digital elevation model (DEM) from the National Elevation Dataset (NED) and a hydrography network from the National Hydrography Dataset (NHD). Soil type distribution and its hydrophysical characteristics (e.g., soil depth, soil hydraulic conductivity, available water capacity) needed to parameterize SWAT's soil database were obtained from STATSGO. A land-use/cover map for the year 2016 at the 30 m resolution was obtained from the National Land Cover Database (NLCD) to characterize the land-use/cover distribution. Daily precipitation, maximum/minimum temperature, relative humidity, wind speed, and short-wave radiation for each subbasin were derived from the GridMet daily gridded dataset (Abatzoglou, 2013) and utilized as weather forcings to drive the hydrological processes in the model. Dry and wet atmospheric deposition of nitrate (NO_3^-) and ammonium (NH_4^+) were obtained from the National Atmospheric Deposition Program for stations AL03, AL10, AL19, and AL99, which fall within the domains of the ACT river basin. Point source discharge information from 90 wastewater treatment plants was downloaded from EPA's ECHO (Enforcement and Compliance History Online) portal and added as point sources to the model. To realistically represent forest dynamics in SWAT, we followed the methodology of Haas et al. (2021) to parameterize FRSE classes. Considering that the vast majority of FRSE consists of loblolly pine in the ACT river basin, we treated all FRSE lands as loblolly pine in SWAT. We initialized the model with FRSE growing in the land from the beginning of the simulation period (IGRO = 1) and deleted all management operations (e.g., planting, fertilization, harvest) attributed to forests by ArcSWAT in the SWAT management file (.mgt). We parameterized initial forest aboveground biomass based on gridded estimates from the United States Department of Agriculture (USDA) Forest Service (Blackard et al., 2008). In the current study, mean annual net primary productivity (NPP) was calculated from simulated forest biomass considering the relationship of 0.45 kg Carbon/kg biomass/m^2 (Tang et al., 2010; Yang and Zhang, 2016).

The complete dataset used for constructing the SWAT model for the ACT river basin, as well as the respective sources, are summarized in Table 2. Based on the described data, SWAT2012 (revision 664) through the ArcSWAT interface with a 10%-10%-0% (land-use, soils, slope) threshold generated 320 subbasins and 4,758 HRUs for the ACT river basin. The model was run from 1979 to 2020, using 3 years (1979-1981) of initialization as the model warm-up period. It is important to note that automated streamflow calibration was not performed in the current study, as our objective is not to optimize streamflow performance but rather to evaluate the significance of forest canopy evaporation in model predictability. However, envisioning to assure that the simulated water budget is reasonable, we built upon the concept of soft data (Yen et al., 2014) and manually adjusted AET rates using remote-sensing estimates from PML-V2 and MOD16A2, besides comparing simulated average annual streamflow at the watershed's most downstream location against observations from the USGS monitoring station 02428400.

Table 2 - Description of the input data utilized to construct the watershed model and evaluate the model performance in simulating streamflow and stream temperature.

Data	**Description**	**Source**

Model input data	Topography	National Elevation Dataset at 10 meters resolution	United States Department of Agriculture (USDA) Geospatial Data Gateway (https://datagateway.nrcs.usda.gov/)
	Land use	2016 NLCD	United States Department of Agriculture (USDA) Geospatial Data Gateway (https://datagateway.nrcs.usda.gov/)
	Soil	State Soil Geographic (STATSGO)	United States Department of Agriculture (USDA) Geospatial Data Gateway (https://datagateway.nrcs.usda.gov/)
	Climate	Daily precipitation, maximum/minimum temperature, solar radiation, and wind speed from 1979 to 2020	GridMet (https://www.climatologylab.org/gridmet.html)
	Atmospheric deposition	Average annual wet and dry deposition of nitrate and ammonia from 1982 to 2020.	National Atmospheric Deposition Program (NADP) (http://nadp.slh.wisc.edu/)
	Point sources	Monthly discharge and loading from wastewater treatment plants from 2007 to 2020	EPA's ECHO Portal (https://echo.epa.gov/trends/loading-tool/get-data/monitoring-data-download)
	Forest Types	National Forest Types for the conterminous U.S.	https://data.fs.usda.gov/geodata/rastergateway/forest_type/index.php
	Forest biomass	Spatially distributed forest aboveground biomass estimates for the conterminous U.S.	https://data.fs.usda.gov/geodata/rastergateway/biomass/conus_forest_biomass.php
Model evaluation	Streamflow	Daily discharge from USGS gage stations 02388500, 02395890, 02411000, 02419890, 02425000, 02428400	USGS Water data (https://waterdata.usgs.gov/nwis)
	ET components (E_i, E_t, E_s)	8-day E_i, E_t, E_s, and ET data from the Penman-Monteith-Leuning Evapotranspiration V2 (PML-V2) product	Google Earth Engine (https://code.earthengine.google.com/d873ae57434c3a78481da819f3cd7bd6)
	Annual NPP	Annual NPP from the MODIS Net Primary Production CONUS dataset	Google Earth Engine (https://code.earthengine.google.com/e8db489c50cabd5db286a7146dfa2775)

2.5. Using gridded data to improve the representation of canopy evaporation in SWAT

In this study, we derived spatially distributed estimates of E_i, transpiration (E_t), and AET from the Penman-Monteith-Leuning Evapotranspiration V2 (PML-V2) product (Zhang et al., 2019) using Google Earth Engine (GEE). The PML-V2 is a gridded ET product that estimates ET and its three components (i.e., E_t, E_i, E_s) at 500 m spatial and 8-day temporal resolutions from 2003 to 2017, making it ideal for watershed-scale applications. The product builds upon the previously developed biophysical model PML-V1 (Zhang et al., 2016) and uses leaf area index (LAI) data from the Moderate Resolution Imaging Spectroradiometer (MODIS), GLDAS meteorological forcing data, atmospheric CO_2 concentrations from the National Oceanic and Atmospheric Administration (NOAA), continuous annual land-use/cover distribution from NASA, among other inputs. The PML-V2 has been calibrated across 95 flux sites worldwide, out of which 22 were ENF and 6 EBF, outperforming widely used products like MOD16A2 (Mu et al., 2013), MOD17A2H (Running et al., 2015) and GLEAM (Global Land Evaporation Amsterdam Model) (Miralles et al., 2011a) in estimating ET and gross primary productivity (GPP).

Here we take advantage of this high-resolution gridded dataset and SWAT's semi-distributed capabilities to constrain the watershed model with spatially distributed estimates of forest E_i and (a) use a data-driven approach to derive physically meaningful values for the input parameter can_{mx} (Eq. 2); (b) calibrate the parameter c in the new canopy interception method (Eq. 11) for forests across a wide geographic range. Since our goal in the current study is to focus on canopy evaporation from forest ecosystems, we selected field-scale sites (Figure 1) covered by FRSE to isolate these ecosystems and thus avoid the confounding effects of other land-use classes when extracting E_i data from PML-V2. To capture a wide geographic range and various environmental conditions, we used the following criteria to select the field-scale sites: (i) be classified as FRSE according to NLCD16, (ii) one field-scale site located within each study watershed, (iii) be entirely located within a single model subbasin, (iv) capture as many physiographic regions as possible, (v) be larger than a 500 X 500m (0.25 km^2) resolution pixel of PML-V2, and (vi) spread across varying elevations.

The rationale utilized to carry out (a) and (b) are explained next.

a. **Field-scale data-driven parameterization**: This approach aimed to inform SWAT with estimates of canopy evaporation from 2003 to 2017 to realistically represent forest canopy storage in the model. To accomplish this, can_{mx} was back-calculated from Eq. 2 by approximating can_{day} as the average daily E_i value derived from PML-V2 at each field-scale site in the period 2003-2017; LAI as the average daily forest LAI simulated by SWAT during the same period; and LAI_{mx} as the input value assigned to the *BLAI* parameter for FRSE in SWAT's plant database. In the current study, an LAI_{mx} value of 3.7 m^2/m^2 was utilized for FRSE classes. To determine LAI in Eq. 2, the average daily simulated LAI from all FRSE HRUs within the subbasins where the field-scale sites are located was calculated.

b. **Field-scale calibration**: Here we used E_i values from PML-V2 as a benchmark to assess the plausibility of SWAT in capturing forest canopy evaporation with the newly introduced canopy interception method. To minimize the differences between simulations and observations and account for landscape heterogeneities (Table 1), annual average forest E_i estimates from PML-V2 for the period 2003-2017 were used to adjust c in Eq. 11 for FRSE at each field-scale site. The model performance in capturing E_i was assessed after each model run based on graphical analyses and statistical rating metrics. Once a good match between simulated and observed E_i was found and no significant improvement in model performance was observed in subsequent model runs, c was considered calibrated for a specific site.

The physical boundaries of each field-scale site illustrated in Figure 1 were uploaded to GEE as shapefiles to extract site-specific estimates of canopy evaporation.

2.6. Experimental design

Modeling experiments were designed and carried out using SWAT to assess the importance of accurately representing canopy interception and evaporation in watershed models. The modeling experiments were as follows.

1. **Default SWAT (M_0)**: SWAT 2012 Rev 664 was setup and run with the default canopy interception and evaporation equations described in section 2.1. Forest canopy storage was parameterized as described in section 2.5.

2. **Modified forest canopy interception (M_{CanInt})**: SWAT 2012 Rev 664 was setup and run with the newly introduced forest canopy interception method explained in section 2.2 and calibrated as described in section 2.5.

M_0 and M_{CanInt} were set up under the same conditions and with the same data explained in section 2.4 - the only difference being how the models handled forest canopy evaporation. Thus, any differences in model predictions are due to forest canopy representation in the model and tell us the relevance of E_i for simulating water yield, sediment yield, ecological flows, nutrient loading, and forest productivity.

2.7. Model performance assessment and evaluation criteria

The performance of M_0 and M_{CanInt} in simulating annual average forest E_i, E_t, and AET from 2003 to 2017 was assessed by comparing model predictions against PML-V2 estimates. For scaling up the model parameterization and calibration of M_0 and M_{CanInt} to the watershed level, the calibrated values of *canmx* and *c*, determined at the field-scale, were applied to all FRSE HRUs within the specific watersheds draining each field-scale site (Figure 1). This resulted in six different parameterizations of *canmx* and *c* across the ACT river basin.

The effects of forest canopy evaporation on the model's prediction of daily streamflow were examined by comparing simulated and observed discharge under M_0 and M_{CanInt} at the outlet of each study watershed. The analysis covered the period of 1982-2020 for the Oostanaula, Etowah, Coosa, Cahaba, and Alabama river watersheds, and 1995-2020 for the Tallapoosa river watershed. Streamflow observations were derived from the USGS stations listed in Table 1. Ecologically relevant flow parameters such as seasonal flows, maximum flows of various durations (i.e., 1, 3, 7, 30, and 90-day), monthly low flows, and timing of maximum and minimum flows were calculated using the Indicators of Hydrologic Alteration (IHA) method (Richter et al., 1996). To accomplish this, we used the desktop model developed by the Nature Conservancy and fed it with daily time series of simulated and observed streamflow. Simulated sediment, nitrate, and organic nitrogen loadings with M_0 and M_{CanInt} in the period 1982-2020 were compared at the outlet of each study watershed. Similarly, model predictions of NPP were compared against the 250 m resolution MODIS Net Primary Production CONUS dataset (Robinson et al., 2018) at each field-scale site shown in Figure 1.

To rate the performances of M_0 and M_{CanInt} in capturing E_i, E_t, and AET, the statistical rating metrics Root Mean Square Error (*RMSE*), percentage bias (*PBIAS*), and coefficient of determination (R^2) were used. These statistical metrics are commonly used to evaluate model performance in capturing biophysical variables such as LAI and AET (Alemayehu et al., 2017; Rajib et al., 2018a; Strauch and Volk, 2013; Yang and Zhang, 2016). The model accuracy in simulating streamflow under M_0 and M_{CanInt} was assessed based on *PBIAS* and the Nash-Sutcliffe Efficiency (*NSE*) coefficient. For detailed information regarding these evaluation criteria, the reader is referred to Althoff and Rodrigues (2021) and Moriasi et al. (2007).

3. Results

3.1. Forest evapotranspiration partitioning

The parameterization of M_0 and calibration of M_{CanInt} resulted in Can_{mx} and c ranges of 0.3-0.55 mm and 0.27-0.5 mm, respectively, across the ACT river basin (Table 3).

Table 3 – Adjusted values of maximum canopy storage (Can_{mx}) and c under M_0 and M_{CanInt}, respectively, at each field-scale study site.

	Can_{mx} (mm)	**c (mm)**
Oostanaula	0.44	0.42
Etowah	0.55	0.46
Coosa	0.30	0.27
Tallapoosa	0.45	0.36
Cahaba	0.40	0.35
Alabama	0.55	0.50

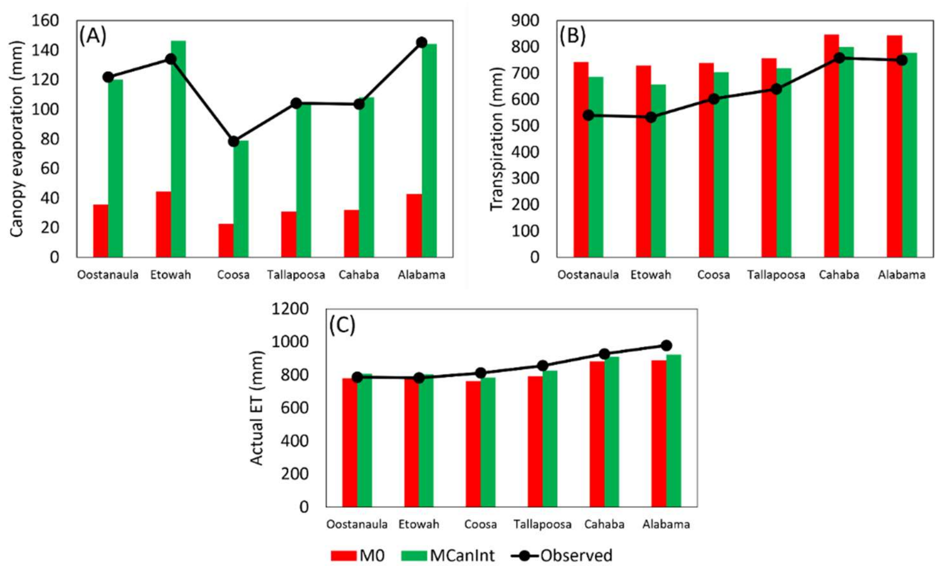

Figure 2 – Simulated versus observed annual average canopy evaporation, transpiration, and total actual ET under M_0 and M_{CanInt} at each field-scale study site from 2003 to 2017.

Considerable differences in simulated average annual forest canopy evaporation in the period 2003-2017 were found between M_0 and M_{CanInt}, with M_0 largely underestimating forest E_i at all study sites (Figure 2A). M_{CanInt} substantially improved the agreement between simulated and PML-V2 estimates of forest E_i at all sites. The average annual forest E_i from PML-V2 across sites was 115 mm for the period 2003-2017. Comparatively, model predictions with M_0 and M_{CanInt} were 35 and 117 mm, respectively, during the same period. The better performance of M_{CanInt} in capturing forest E_i is corroborated by the statistical rating metrics shown in Table 4. *PBIAS* ranged from 67 to 71% with M_0 and from -9 to 1.4% with M_{CanInt}, confirming the large underestimation of forest E_i achieved with the default SWAT model and the slight overestimation yielded by our proposed approach. A better fit between simulations and observations was found with M_{CanInt}, as confirmed by the R^2 and *RMSE* ranges of 0.09-0.45 and 11-24 mm, respectively, as opposed to the 0.07-0.44 and 56-103 mm obtained with M_0.

The effects of forest E_i modeling on simulated forest E_t and AET were modest but, overall, resonated in improved predictions under M_{CanInt} compared to M_0 (Figure 2B-C). SWAT overestimated forest E_t under both model configurations, although M_{CanInt} led to reduced overestimations compared to M_0. While the average annual forest E_t from PML-V2 was 637 mm during the 2003-2017 period, M_0 and M_{CanInt} estimates were 777 and 724 mm, respectively. The average *PBIAS* was reduced from -23% (M_0) to -15% (M_{CanInt}), whilst mean R^2 and *RMSE* changed from 0.17 (M_0) to 0.15 (M_{CanInt}), and from 179 (M_0) to 140 (M_{CanInt}) mm.

Conversely, forest AET was underestimated under M_0 and M_{CanInt}, with average annual values of 813 and 842 mm, respectively, compared to the 857 mm of PML-V2 estimates. M_{CanInt} significantly reduced the underestimation of average annual forest AET and better matched the PML-V2 values. *PBIAS* ranged from 0.76 to 9% with M_0 and from -3 to 6% with M_{CanInt}, with mean values across sites of 5 and 2%, respectively. The mean R^2 values across sites increased from 0.18 to 0.22 with M_{CanInt}, whilst the mean *RMSE* across sites was 118 mm for both model configurations in simulating forest AET.

Time-series of annual average simulated versus observed forest E_i, E_t, and AET for the period 2003-2017 are shown for each field-scale site in the Supplementary Materials file (Figures S2-S7).

Table 4 – Statistical rating metrics of simulated annual average canopy evaporation, transpiration, and total actual ET at each field-scale study site from 2003 to 2017. Positive PBIAS values indicate model underestimation, while negative PBIAS values indicate model overestimation.

		Canopy evaporation		**Transpiration**		**Actual ET**	
		M_0	**M_{CanInt}**	**M_0**	**M_{CanInt}**	**M_0**	**M_{CanInt}**
Oostanaula	R^2	0.44	0.45	0.03	0.01	0.06	0.09
	PBIAS (%)	71	1.4	-38	-27	0.76	-2.7
	RMSE (mm)	87	15	218	165	85	95
Etowah	R2	0.38	0.34	0.18	0.10	0.14	0.17
	PBIAS (%)	67	-9	-37	-23	1	-3
	RMSE (mm)	91	24	214	146	81	89
Coosa	R2	0.32	0.34	0.14	0.14	0.18	0.23
	PBIAS (%)	71	-1	-22	-17	6	3
	RMSE (mm)	56	11	178	154	129	128
Tallapoosa	R2	0.09	0.09	0.28	0.30	0.23	0.32
	PBIAS (%)	70	-1	-18	-12	8	4
	RMSE (mm)	74	16	157	131	124	118
Cahaba	R2	0.07	0.11	0.28	0.25	0.27	0.29

	PBIAS (%)	69	-5	-12	-6	5	2
	RMSE (mm)	72	17	160	137	139	138
Alabama	R2	0.09	0.10	0.22	0.24	0.10	0.07
	PBIAS (%)	70	1	9	6	-13	-4
	RMSE (mm)	103	22	151	140	148	110

3.2. Water availability

Beyond improving E_t and AET predictions, M_{CanInt} also translated into differences in all components of water balance partitioning compared to M_0. The changes in average annual surface runoff (SQ), lateral flow (LQ), baseflow (GW), and AET brought about by the implementation of M_{CanInt} are illustrated in Figure 3 for the period 1982-2020. In forested areas, an average decrease of 36% in SQ was found across the ACT river basin, with the Etowah (48%) and Coosa (30%) river watersheds witnessing the biggest and smallest changes, respectively. Differences in annual LQ and GW between M_0 and M_{CanInt} were small, with average decreases of 4%. On average, forest AET increased by 4% with the implementation of M_{CanInt}.

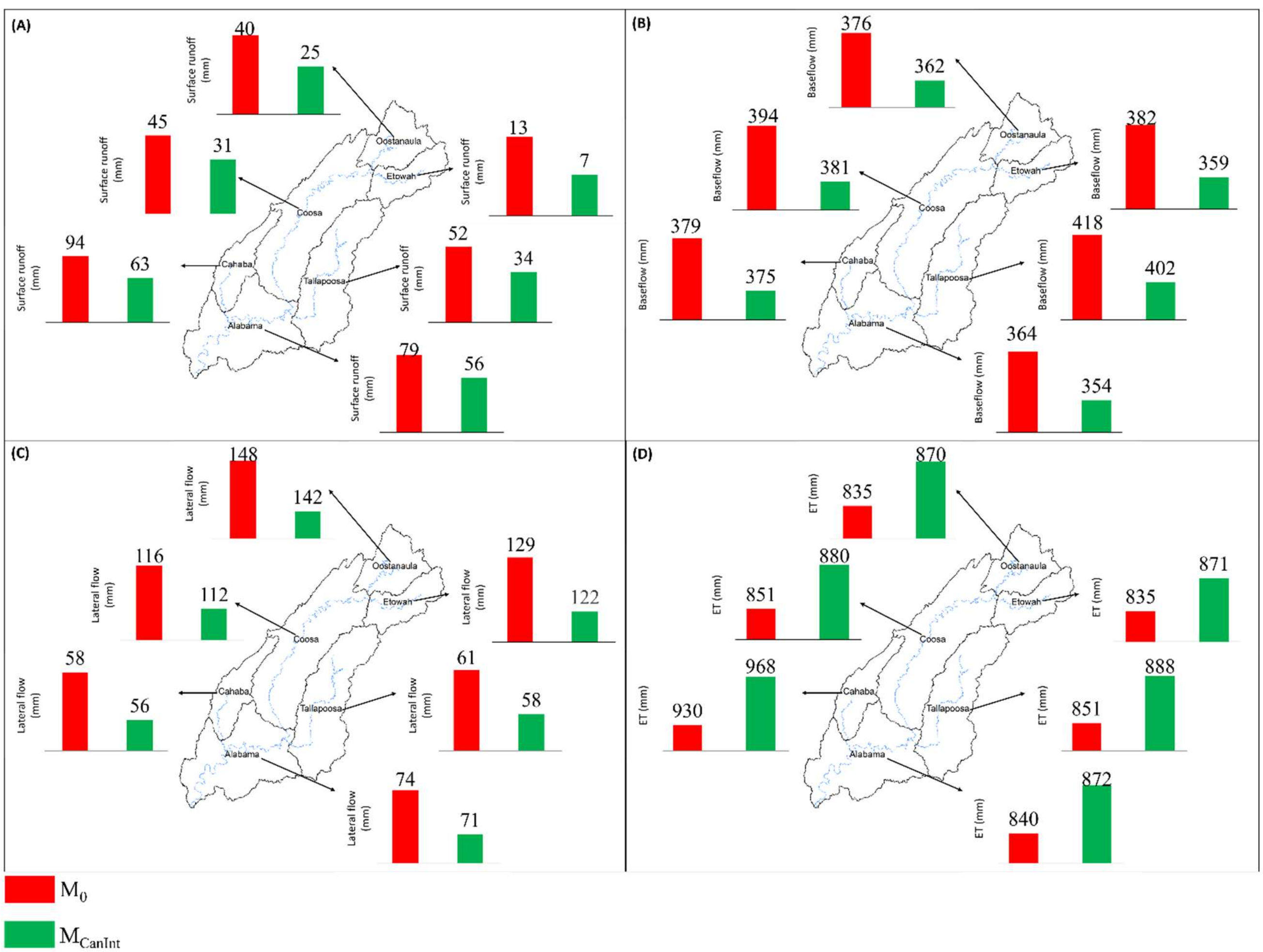

Figure 3 – Water balance partitioning from 1982 to 2020 under M_0 and M_{CanInt} across all study watersheds considering forest HRUs only. Water balance is partitioned into surface runoff (A), baseflow (B), lateral flow (C), and AET (D).

Furthermore, the modified model led to enhanced daily streamflow predictions at all study watersheds compared to the default version of SWAT (Figure 4). The temporal agreement between simulated and observed streamflow improved with M_{CanInt}, as indicated by the *NSE* values illustrated in Figure 4A-B, which jumped from a range of -1.25 to 0.64 under M_0 to a range of -1.13 to 0.68 under M_{CanInt}. Overall, streamflow performance increased from lower to higher stream orders under both model configurations across the ACT river basin, and negative *NSE* values were only found at the upstream Oostanaula and Etowah river watersheds. Individual flow duration curves (FDCs) for each study watershed are provided in the Supplementary Materials file (Figure S15-S20) and may help to illustrate the changes in simulated daily streamflow brought about M_{CanInt}. SWAT overestimated medium flows (flows equaled or exceeded 20-70% of the time) and high flows (flows equaled or exceeded 0-20% of the time), but the implementation of M_{CanInt} reduced this overestimation and improved the agreement with observations across all tested watersheds.

The reduced model overestimation of daily streamflow achieved by M_{CanInt} is supported by the *PBIAS* values shown in Figure 4C-D. Overall, SWAT largely overestimated streamflow across the ACT river basin, with *PBIAS* ranges of -38% to -1% and -31% to -4% under M_0 and M_{CanInt}, respectively, and mean values of -25% and -19%. Notably, M_{CanInt} outperformed M_0 in capturing streamflow at all watersheds, with marked differences found in the upstream Oostanaula and Etowah River watersheds. In these areas, PBIAS changed from -38 to -31%, and from -37 to -31%, respectively. The Cahaba River watershed also witnessed a significant reduction in *PBIAS* for streamflow simulation from the M_0 (-36%) to the M_{CanInt} (-29%) modeling condition.

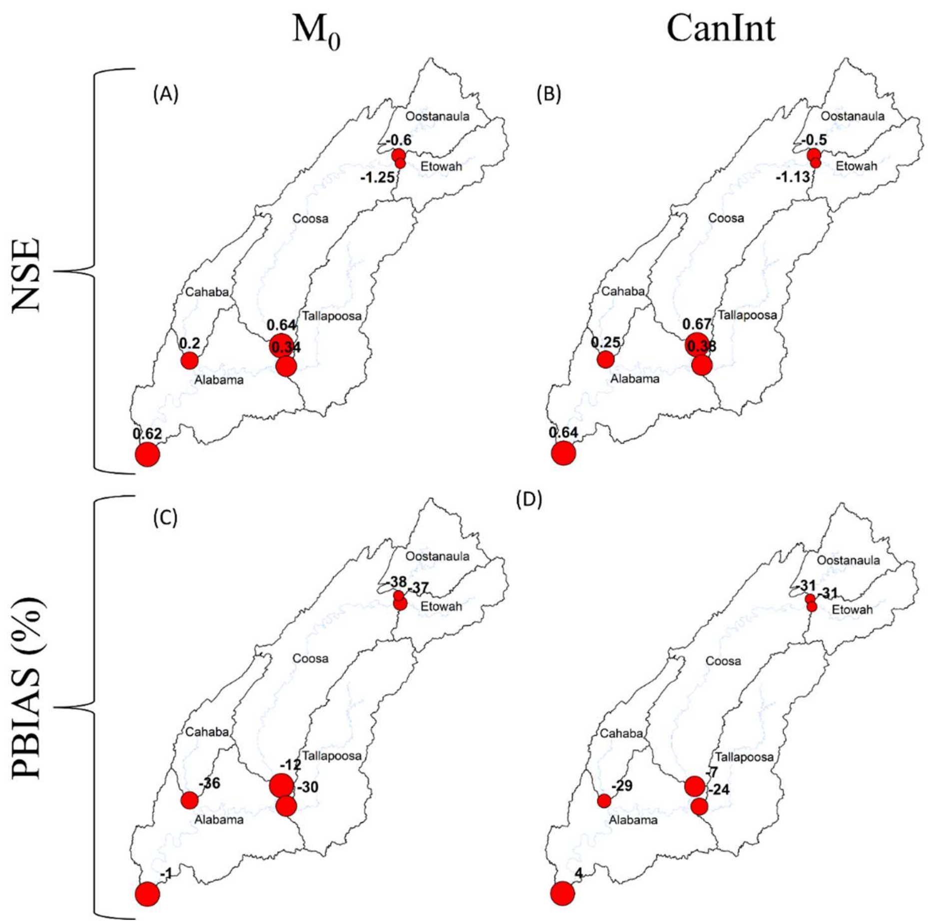

Figure 4 – Model performance in simulating daily streamflow under M_0 and M_{CanInt} across all study watersheds.

3.3. Ecological flows

Figures 5-8 summarize the hydrological alteration induced by forest canopy representation in SWAT. Each figure shows the percentage difference between simulations and observations considering different ecologically relevant flow metrics. Monthly low flows were substantially overestimated by M_0, with overestimations ranging from 18 to 99% (Figure 5). Simulated monthly low flows with M_{CanInt} had better agreement with observations across all sites, with model overestimation reduced to the range of 12-84%.

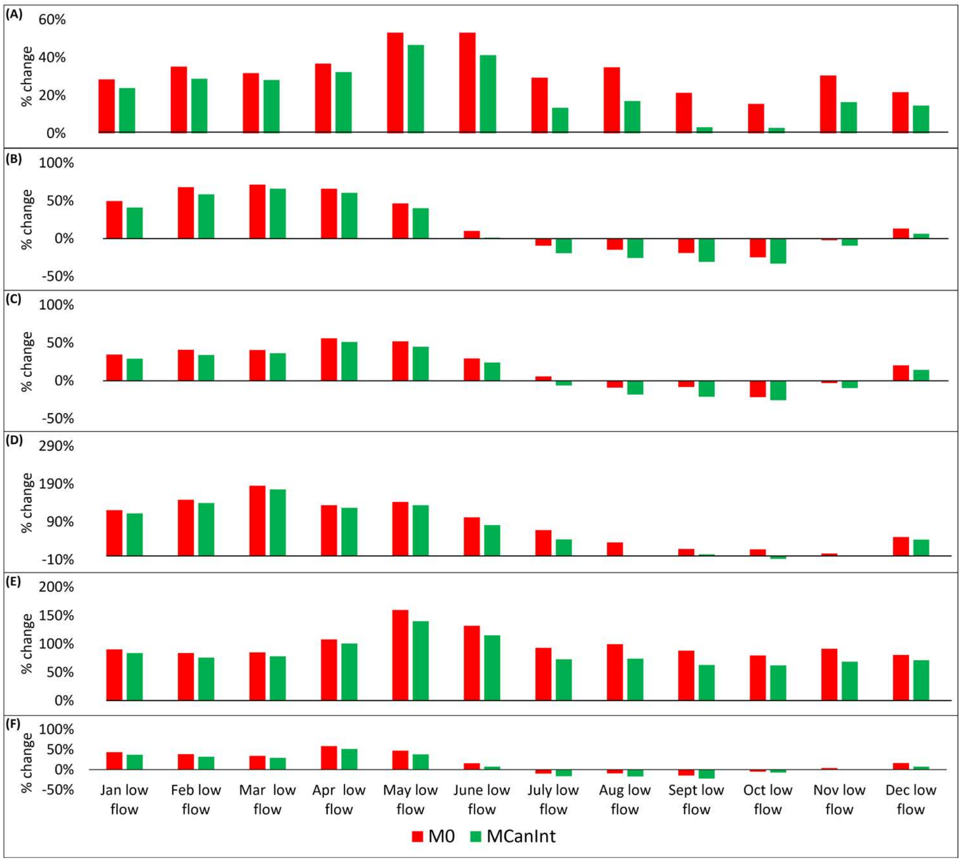

Figure 5 – Percent difference between observed and simulated monthly low flows with the default (M_0) and modified (M_{CanInt}) SWAT models at the outlet of the Oostanaula (A), Etowah (B), Coosa (C), Tallapoosa (D), Cahaba (E), and Alabama (F) watersheds.

Figure 6 illustrates maximum flows of daily (1-day), weekly (3-day, 7-day), monthly (30-day), and seasonal (90-day) durations simulated under M_0 and M_{CanInt}. Overall, SWAT overestimated maximum flows under M_0 and M_{CanInt}. Exceptions were found at the Tallapoosa and Cahaba watersheds, where the model slightly underestimated maximum flows of 1 to 30-day duration. However, with M_{CanInt} the model overestimation was alleviated at most sites and resonated in better agreement with observations. Mean model overestimation of maximum flows was in the ranges of 3-78% and 1-75% with M_0 and M_{CanInt}, respectively.

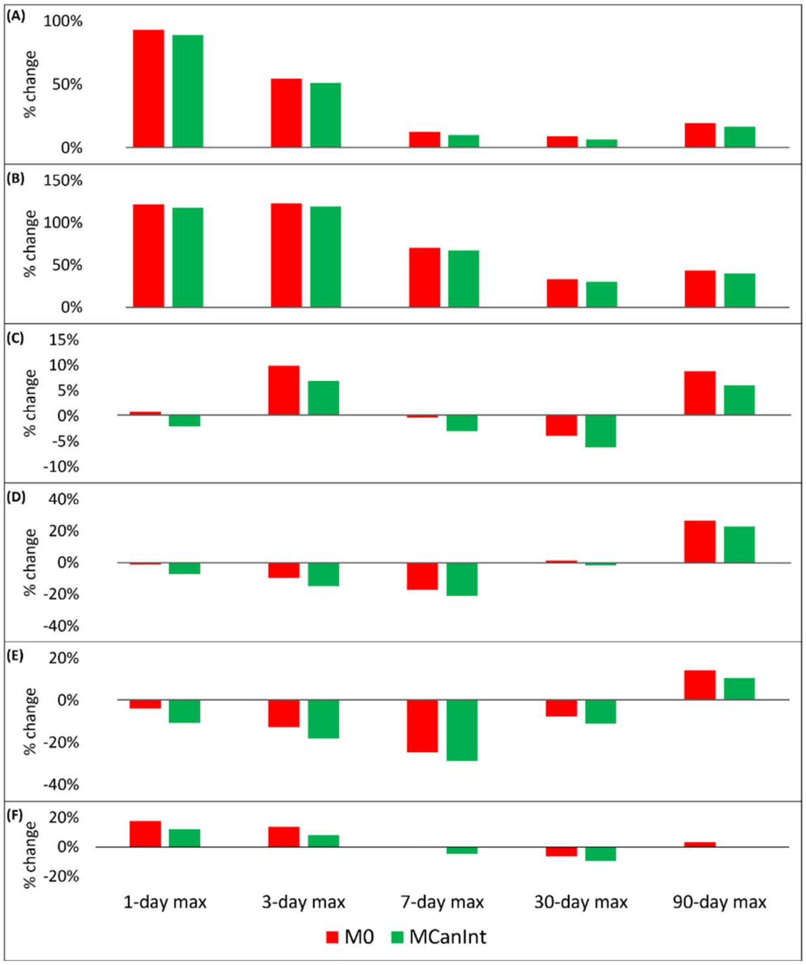

Figure 6 - Percent difference between observed and simulated maximum flows of various durations with the default (M_0) and modified (M_{CanInt}) SWAT models at the outlet of the Oostanaula (A), Etowah (B), Coosa (C), Tallapoosa (D), Cahaba (E), and Alabama (F) watersheds.

Simulated seasonal flows showed significant variations across sites (Figure 7). At the Etowah, Coosa, and Alabama watersheds, SWAT largely underestimated spring and summer flows, whilst slightly overestimating streamflow in the winter and fall. At these sites, M_{CanInt} had poorer performance compared to M_0. At the Oostanaula, Tallapoosa, and Cahaba watersheds, SWAT overestimated seasonal flows, with model overestimations in the range of 17-70% and 8-59% with M_0 and M_{CanInt}, respectively.

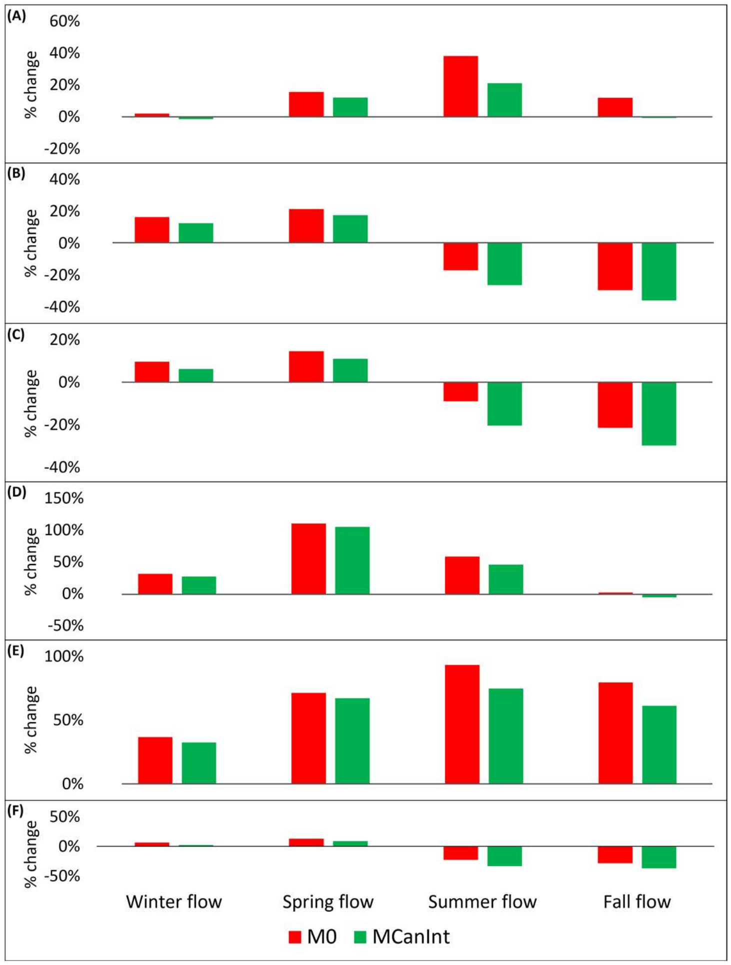

Figure 7 - Percent difference between observed and simulated seasonal flows with the default (M_0) and modified (M_{CanInt}) SWAT models at the outlet of the Oostanaula (A), Etowah (B), Coosa (C), Tallapoosa (D), Cahaba (E), and Alabama (F) watersheds.

The Julian dates of maximum and minimum flows were also impacted by forest canopy evaporation across our study sites (Figure 8). No changes in the timing of minimum flows were found in the Tallapoosa and Alabama watersheds. In the Oostanaula, Etowah, Coosa, and Cahaba watersheds, the date of minimum flows was slightly different between M_0 and M_{CanInt}, with M_0 better matching the observations. Overall, the date of minimum flow predicted by M_0 and M_{CanInt} were 16-22 days and 19-25 days earlier, respectively, compared to the observed flow. The date of maximum flow was only changed in the Cahaba and Alabama watersheds, where M_{CanInt} had significantly better agreement with observations. At these watersheds, the date of maximum flow predicted by M_0 and M_{CanInt} were 21-46 days and 18-22 days later, respectively, compared to the observations.

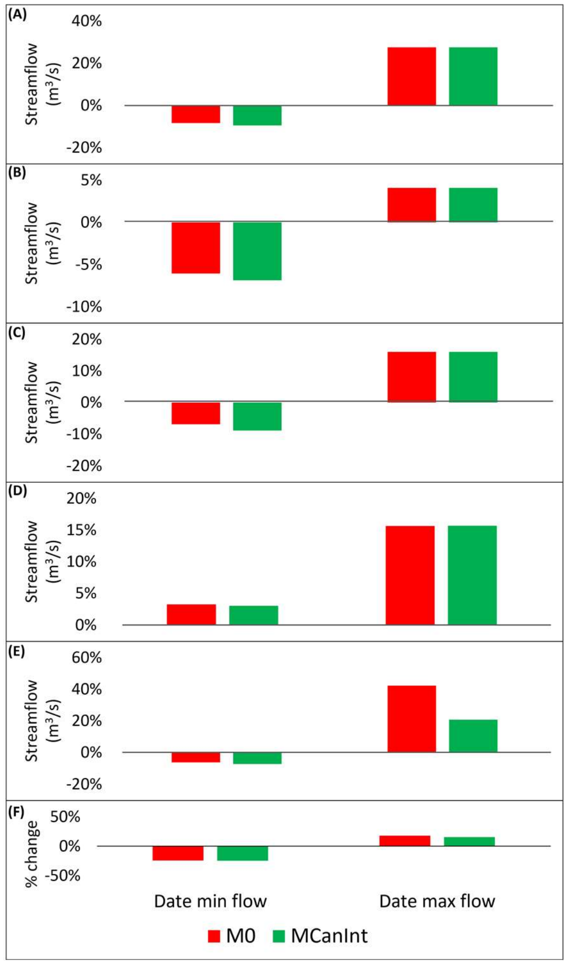

Figure 8 - Percent difference between observed and simulated Julian date of maximum and minimum flows with the default (M_0) and modified (M_{CanInt}) SWAT models at the outlet of the Oostanaula (A), Etowah (B), Coosa (C), Tallapoosa (D), Cahaba (E), and Alabama (F) watersheds.

3.4. Sediment yield and nutrient loading

The representation of canopy evaporation had important implications for soil erosion and nutrient retention across the ACT river basin in the period 1982-2020 (Figure 9). Overall, M_{CanInt} led to reduced average annual loadings of sediment, nitrate (NO_3^-), and organic nitrogen at all study watersheds compared to M_0. Notably, sediment and organic nitrogen loadings experienced the most substantial changes, with average reductions of 13 and 11%, respectively. Nitrate loadings were reduced by 5% with M_{CanInt} in relation to M_0. For all water quality variables shown in Figure 9, the biggest and smallest changes were observed in the Tallapoosa and Etowah river watersheds.

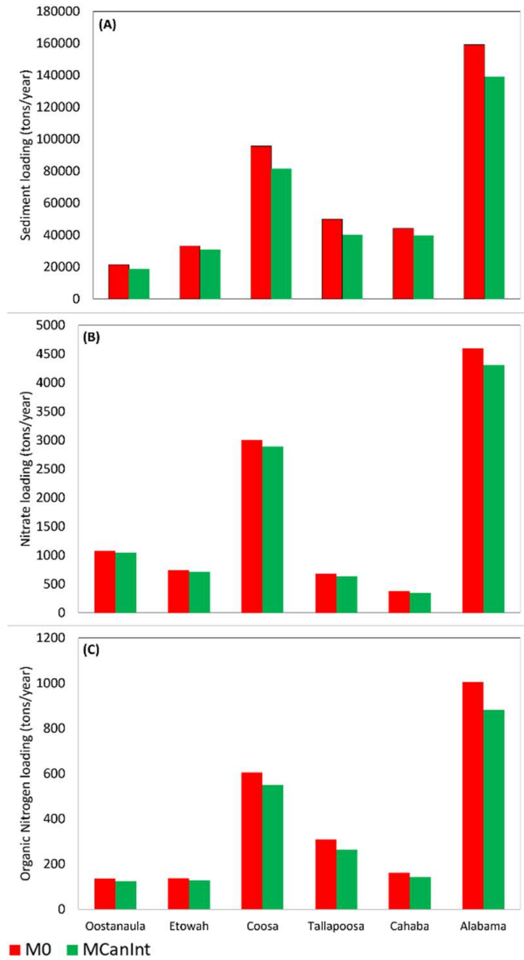

Figure 9 – Effects of forest canopy evaporation on simulated sediments (A), nitrate (B), organic nitrogen (C), phosphate (D), and total organic carbon (E) loadings at the watershed outlet.

3.5. Ecosystem productivity

Forest NPP was largely overestimated by M_0 and M_{CanInt} across all study sites (Figure 10). NPP estimates derived from MODIS CONUS in the period 2001-2020 ranged from 7,692 to 8,415 kgC/m^2/year, with the highest and lowest values found at the Oostanaula and Cahaba watersheds, respectively. Simulated NPP with M_0 and M_{CanInt} was in the range of 12,354-15,096 kgC/m^2/year and 12,143-14,312 kgC/m^2/year, respectively. The highest and lowest simulated NPP was found at the Tallapoosa and Cahaba watersheds, respectively. Although both M_0 and M_{CanInt} substantially overestimated MODIS CONUS NPP, model predictions under M_{CanInt} had slightly better agreement with benchmark data. Under M_0, model overestimation of forest NPP ranged from 50-87%, whilst it was mitigated to 48-86% with M_{CanInt}.

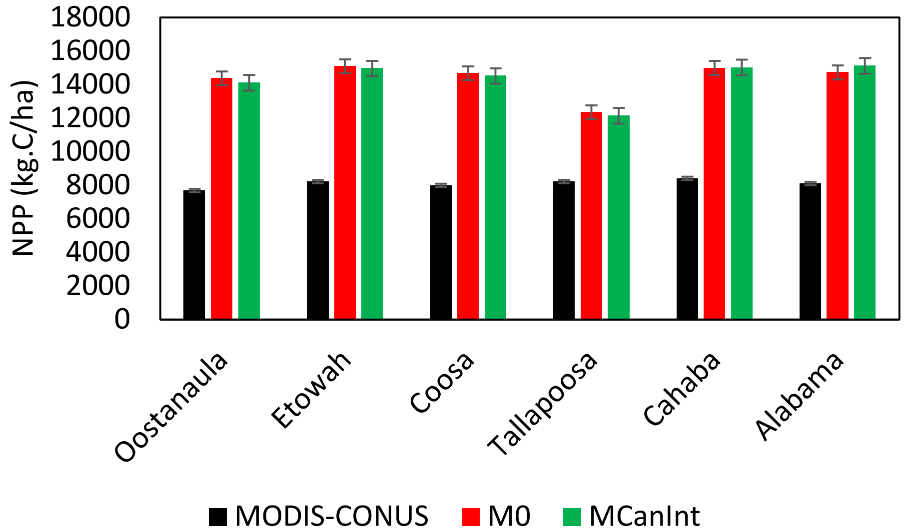

Figure 10 – Comparison of default and modified SWAT simulations of forest net primary productivity against remote-sensing estimates at six study sites in the period 2001-2020.

4. Discussion

In the face of climate and land-use changes, it is imperative to improve the mechanistic understanding of the ecosystem functions in ecohydrological models for developing sustainable adaptation and mitigation scenarios. Models can be used to inform environmental policy decisions by presenting different courses of action. However, accurate model parameterization, assumptions, and input data are key for achieving reliable results.

4.1. Improved forest evapotranspiration partitioning

Our findings reveal that data-driven parameterization was not effective in capturing forest canopy evaporation (E_i) with the SWAT model across all study sites. This indicates that the internal model structure in representing canopy rainfall interception and evaporation in forest ecosystems might be imprecise in SWAT. Studies such as Yang et al. (2018) and Haas et al. (2022) have shown that SWAT underestimates actual evapotranspiration (AET) in forest ecosystems and attributed this to unrealistic model parameterization of processes such as stomatal conductance, and minimum and maximum LAI. Our results demonstrate that the default representation of E_i in SWAT (M_0) led to large underestimations of canopy evaporation at forested sites compared to gridded remote-sensing data. After implementing minor changes to the model's source code, model estimates of forest canopy evaporation showed much better agreement with benchmark data, leading to an overall slight overestimation. This agrees with Kofroňová et al. (2021), which demonstrated that even simple interception models, under the right assumptions, can improve the performance of hydrologic models in forest ecosystems. The main reason why SWAT misrepresented forest E_i with its default formulation is most likely because the model uses the same equation to compute E_i for all types of plants (Eq. 2). In SWAT, canopy interception is calculated as a function of canopy storage and plant LAI and is normalized by the maximum attainable plant LAI. Since the plant growth module of SWAT is based on the EPIC crop growth model, it may not be ideal for forests and some processes such as canopy evaporation, which vary from short to tall vegetation, may not be realistically represented. Under our proposed approach (M_{CanInt}), we eliminated the maximum LAI normalization and calculated canopy rainfall interception for forests as a linear function of LAI and a user-defined parameter *c*. The same approach has been used in land surface models such as the Canadian Land Surface Scheme and the Community Land Model (CLM); as well as in field studies (Amatya et al., 1996; J. McCarthy et al., 1991; Spittlehouse and Black, 1981). Although widely used, this method is very simplistic, and *c* needs to be adjusted to accurately capture forest E_i across the landscape. The value of *c* has been commonly assumed as 0.2 based on the studies of Rutter (1975) and Dickinson (1987). However, as highlighted by Hadiwijaya et al. (2021), further research is needed on the relationship between canopy storage and *c*. In the current study, we used gridded estimates of forest E_i to calibrate *c* for evergreen forests across the ACT river basin and found a range of 0.27-0.50. Improved forest E_i led to cross-benefits in terms of forest transpiration (E_t) and AET across all study sites. Under M_0, E_t and AET were over and underestimated, respectively, because of underestimated E_i. Under M_{CanInt}, as a result of increased E_i, E_t and AET were reduced and increased, respectively, leading to both having better agreements with benchmark data. Simulated AET with M_{CanInt} concurred well with AET ranges across the southeast United States (SE-US). For instance, McLaughlin et al. (2013) reported annual AET varying from 838 to 1,087 mm for loblolly pine stands in the SE-US, agreeing well with the 842 mm of mean AET achieved with M_{CanInt} and diverging from the 813 mm yielded by M_0. Our results suggest that the underestimation of AET in forest ecosystems found by past SWAT studies might be related to a large underestimation of canopy evaporation.

The E_i/P ratios simulated by M_{CanInt} across FRSE HRUs varied from 0.07 to 0.11, showing reasonable agreement with other studies. For instance, Gu et al. (2018) found an average global E_i/P ratio of 0.12 for evergreen needleleaf forests (ENF). Miralles et al. (2011) found a much larger global E_i/P value of 0.22. Crockford and Richardson (2000) reported E_i/P ratios of 0.16 for ENF in Australia. Under M_0, E_i/P ratios varied from 0.02 to 0.04, showing a substantial underestimation of watershed-averaged forest E_i compared to the published literature. The small increase in AET, despite large increases in canopy evaporation, may be explained by how the evapotranspiration demand is handled in SWAT. The AET demand is sequentially met by canopy evaporation, transpiration, and soil evaporation, where increasing evaporation from one of these pools resonates with decreased evaporation from the others. In our case, by increasing canopy evaporation, transpiration was reduced. The overall consequence was a modest increase in AET across the study sites.

4.2.Implications for water quantity modeling

The increased evapotranspiration yielded by M_{CanInt} translated into small decreases in annual water yield compared to M_0. This was expected since more water was lost to the atmosphere as vapor in M_{CanInt}, which resulted in less water eventually becoming surface runoff, lateral flow, and baseflow. In forested areas, mean annual surface runoff was impacted the most and witnessed decreases in the range of 6-33 mm with M_{CanInt} across our study watersheds. Reduced water yield simulated by M_{CanInt} resonated in less in-stream fluxes compared to M_0, as shown by the reduced *PBIAS* values when comparing simulated and observed daily streamflow across the study watersheds. Results showed that the model performance in capturing streamflow improved with M_{CanInt}, indicating that there is a cross-benefit of our improved forest E_i method for simulating streamflow in watershed models. The improved streamflow performance was more evident in the Cahaba and Tallapoosa River watersheds. This is not surprising considering that these watersheds have the highest FRSE coverage among all study watersheds (Table 1). Our findings are in line with other studies showing the benefits of constraining ecohydrological models with biophysical variables such as LAI (Alemayehu et al., 2017;

Rajib et al., 2020, 2018a; Strauch and Volk, 2013), AET (Parajuli et al., 2018; Tobin and Bennett, 2017), soil moisture (Rajib et al., 2016), and transpiration (Li Zejun et al., 2020).

M_{CanInt} outperformed M_0 in capturing ecological flows. Ecologically relevant flow metrics such as maximum flows, monthly low flows, seasonal flows, and the timing of extreme flows can significantly impact the aquatic biota. For instance, fish species of ecological relevance for Alabama such as largemouth bass (*Micropterus salmoides*) thrive in slow-flowing waters, while species like darters (*Etheostoma ranseyi*) prefer swift-flowing waters (Atkins et al., 2004). Additionally, these flow metrics can influence channel morphology and physical habitat conditions. For instance, maximum flows can affect the volume of nutrient exchanges between the channel and floodplains and the distribution of plant communities in lakes, ponds, and floodplain areas. Similarly, monthly low flows sustain aquatic life in dry spells by ensuring a minimum water level in the channel and floodplains. Seasonal flows align with species' reproductive and feeding cycles, preserving and maintaining aquatic biodiversity, besides influencing water temperature and oxygen levels (Richter et al., 1996). Also, better predicting the timing of maximum and minimum flow events can aid in infrastructure planning, flood/drought mitigation, and sustainable water allocation. Thus, accurately simulating these ecological flow metrics might be essential for supporting biodiversity and the overall health of water-dependent ecosystems.

Had the Green-Ampt method had been used to calculate surface runoff in SWAT, the impacts on water availability and ecological flows would most likely have been greater since the redistribution of gross rainfall would be directly affected by canopy interception (Eq. 6). However, running the model with the Green-Ampt formulation requires sub-daily climate data, which may be difficult to obtain, and is thus beyond the scope of the current study and must be explored in a future effort. Under the utilized NRCS-CN method to compute surface runoff, canopy evaporation is lumped together with the initial abstractions term in SWAT (Neitsch et al., 2011). In other words, surface runoff is solely affected by rainfall and the CN value, with canopy evaporation not directly impacting surface runoff generation in SWAT. Thus, the changes in water yield observed between M_0 and M_{CanInt} are a byproduct of increased initial abstractions and consequent reduced surface runoff.

4.3. Implications for water quality and ecosystem productivity modeling

The implementation of M_{CanInt} led to reduced loadings of sediment, nitrate, and organic nitrogen, compared to M_0. The most substantial changes were observed for sediment and organic nitrogen predictions, where a reduction of approximately 8,900 and 1,300 tons/year was found, respectively. This is most likely related to the amounts of residue on the ground produced by M_0 and M_{CanInt}. In SWAT, a fraction of the total forest biomass is assigned to the ground as residue during dormancy. This plant residue contributes to the fresh organic nitrogen pool and is eventually mineralized into NO_3^-. Due to the decreased forest transpiration rates predicted under M_{CanInt}, forest biomass was slightly smaller compared to M_0 (Figure S21). As a result, less fresh residue was assigned to the soil with M_{CanInt}, which can explain the decreases in organic nitrogen and NO_3^-loadings. Similarly, sediment yield is affected by the amount of residue on the soil surface in SWAT since the cover and management factor of the Universal Soil Loss Equation (USLE) (Williams, 1975) is computed as a function of plant residue (Neitsch et al., 2011). Therefore, inaccurate representation of E_i could have implications for studies aimed at simulating nutrient cycling or assessing the impacts of management practices (e.g., forest thinning) on water quality with SWAT. These findings are relevant since studies such as Atkins et al. (2004) and Johnson et al. (2002) highlight the large nitrogen, phosphorous, and carbon loads being transported to the Mobile Bay estuary from agricultural lands and animal wastes.

Similarly, according to Deutsch (2019), soil erosion is the main source of water impairment across the Mobile Bay watershed. Additionally, the modified model positively affected ecosystem productivity through the simulation of NPP, where M_{CanInt} had better agreement with remote-sensing NPP compared to M_0. NPP is an important metric in understanding the flow of energy through ecosystems and is essential for assessing ecosystem health and functioning (Zhang et al., 2023).

4.4. Caveats and broader implications

Our study has limitations, and our results should be interpreted with caution. Although our proposed approach is tailored to forest ecosystems and was applied to all types of forests across the study domain, we focused our model calibration efforts on evergreen forests. Other important forest species (e.g., white/red oaks) like deciduous forests were not parameterized with the same level of detail and that should be addressed in a future study. Additionally, model simulated zero canopy evaporation from non-forested lands, which is a consequence of unrealistic parameterization of canopy storage (*canmx.hru*) in SWAT. This should serve as an alert for future model applications aimed at estimating evapotranspiration partitioning of non-forested lands with SWAT. Despite these shortcomings, our study demonstrates the usefulness of remote-sensing data for informing ecohydrological models in better capturing ecohydrological processes such as forest canopy evaporation. This is relevant given that canopy evaporation represents a big portion of the AET in forest ecosystems. AET, in turn, usually dominates the water budget with a mean global AET/P ratio of 0.6 (Alton et al., 2009; Oki and Kanae, 2006). Additionally, as demonstrated here, the representation of canopy evaporation may have consequences for simulating ecosystem functions and management, such as soil erosion control, nutrient retention, flood and drought management, and forest productivity with SWAT. Thus, adequately representing canopy evaporation in ecohydrological models can be important for strengthening their reliability and in estimating ecological processes of underlying consequences for aquatic species and ecosystem biodiversity. Under our proposed approach, the model can uniquely simulate canopy evaporation for short and tall vegetation, better reflecting real-world conditions. The newly introduced parameter c was calibrated across a wide geographic range of land-use distributions, soil types, elevation profiles, and hydrological conditions (Table 1). Therefore, our findings can also be useful to ecosystem modelers since land surface models such as CLM rely on approaches similar to M_{CanInt} to estimate canopy evaporation. Our model modifications are simple, and the compiled source code is readily available, making our findings broadly useful to the modeling community.

Conclusions

In the current study, we modified the canopy interception and evaporation method used in the SWAT model to better represent forest ecosystems. The following summarizes the main findings of our study:

- The default representation of canopy evaporation in SWAT may be conceptually flawed for forest ecosystems.
- SWAT, under its default formulation, underestimated forest canopy evaporation across all study sites.
- Forest transpiration and actual evapotranspiration (AET) were over and underestimated, respectively, by the default SWAT model.
- The modified model showed better agreement with benchmark data in capturing canopy evaporation.

- Model performance for forest transpiration and AET slightly improved because of improved canopy evaporation.
- Average annual water yield decreased due to increased AET.
- The proposed approach led to reductions in sediment, organic nitrogen, and nitrate loadings compared to the default SWAT.
- Forest net primary productivity was impacted, with the proposed approach reducing model overestimation of benchmark data.

Remote-sensing estimates of canopy evaporation were vital in improving the model. Although our study is in the context of SWAT, our findings can be broadly useful to the modeling community since other popular process-based models like EPIC, APEX, and ALMANAC are based on very similar modeling assumptions. Thus, our methodology can be easily applied to other watershed models and be explored across a wide range of environmental conditions. Due to the divergent simulation of canopy evaporation and ecological processes between the two model configurations, the conclusions drawn from each model could vary considerably. As a result, such discrepancies could potentially influence management decisions if these models were utilized to inform decision-making. Amid ongoing climate and land-use changes, modeling tools capable of accurately capturing ecological processes become invaluable to assess potential mitigation scenarios (e.g., forest thinning, reforestation). Our findings demonstrate the benefits of the modified model not only in predicting forest canopy evaporation but also in cross-benefiting multiple ecological processes, thereby holding implications for aquatic species and ecosystem biodiversity.

Declaration of competing interest

The authors declare that they have no known competing financial interests or personal relationships that could have appeared to influence the work reported in this paper.

Data availability

The executable file of the compiled modified source code can be downloaded from https://github.com/HaasHen/SWAT-Canopy-Interception. The Google Earth Engine scripts developed to derive remote-sensing canopy evaporation, transpiration, total evapotranspiration, and net primary productivity are available in Table 1.

Declaration of generative AI and AI-assisted technologies in the writing process

During the preparation of this work, the author(s) used ChatGPT to improve the writing. After using this tool/service, the author(s) reviewed and edited the content as needed and take(s) full responsibility for the content of the publication.

Acknowledgments

This paper is a result of research funded by the National Oceanic and Atmospheric Administration's RESTORE Science Program under award NA19NOS4510194 to Auburn University.

References

Abatzoglou, J.T., 2013. Development of gridded surface meteorological data for ecological applications and modelling. International Journal of Climatology 33, 121–131. https://doi.org/10.1002/joc.3413

Alemayehu, T., van Griensven, A., Bauwens, W., 2017. Improved SWAT vegetation growth module for tropical ecosystem. Hydrol. Earth Syst. Sci. Discuss. 1–32. https://doi.org/10.5194/hess-2017-104

Althoff, D., Rodrigues, L.N., 2021. Goodness-of-fit criteria for hydrological models: Model calibration and performance assessment. Journal of Hydrology 600, 126674. https://doi.org/10.1016/j.jhydrol.2021.126674

Alton, P., Fisher, R., Los, S., Williams, M., 2009. Simulations of global evapotranspiration using semiempirical and mechanistic schemes of plant hydrology. Global Biogeochemical Cycles 23. https://doi.org/10.1029/2009GB003540

Amatya, D.M., Skaggs, R.W., Gregory, J.D., 1996. Effects of controlled drainage on the hydrology of drained pine plantations in the North Carolina coastal plain. Journal of Hydrology 1–4, 211–232.

Angela, C.-B., Javier, C.-J., Teresa, G.-M., Marisa, M.-H., 2015. Hydrological evaluation of a peri-urban stream and its impact on ecosystem services potential. Global Ecology and Conservation 3, 628–644. https://doi.org/10.1016/j.gecco.2015.02.008

Arnold, J.G., Kiniry, J.R., Srinivasan, R., Williams, J.R., Haney, E.B., Neitsch, S.L., 2011. Soil and Water Assessment Tool Input/Output File Documentation Version 2009. Grassland, Soil and Water Research Laboratory - Agricultural Research Service Blackland Research Center - Texas AgriLife Research.

Arnold, J.G., Srinivasan, R., Muttiah, R.S., Williams, J.R., 1998. Large Area Hydrologic Modeling and Assessment Part I: Model Development1. JAWRA Journal of the American Water Resources Association 34, 73–89. https://doi.org/10.1111/j.1752-1688.1998.tb05961.x

Atkins, J.B., Zappia, H., Robinson, J.L., McPherson, A.K., Moreland, R.S., Harned, D.A., Johnston, B.F., Harvill, J.S., 2004. Water quality in the Mobile River Basin, Alabama, Georgia, Mississippi, and Tennessee, 1999-2001 (USGS Numbered Series No. 1231), Water quality in the Mobile River Basin, Alabama, Georgia, Mississippi, and Tennessee, 1999-2001, Circular. U.S. Geological Survey. https://doi.org/10.3133/cir1231

Bekele, E.G., Lant, C.L., Soman, S., Misgna, G., 2013. The evolution and empirical estimation of ecological-economic production possibilities frontiers. Ecological Economics 90, 1–9. https://doi.org/10.1016/j.ecolecon.2013.02.012

Blackard, J.A., Finco, M.V., Helmer, E.H., Holden, G.R., Hoppus, M.L., Jacobs, D.M., Lister, A.J., Moisen, G.G., Nelson, M.D., Riemann, R., Ruefenacht, B., Salajanu, D., Weyermann, D.L., Winterberger, K.C., Brandeis, T.J., Czaplewski, R.L., McRoberts, R.E., Patterson, P.L., Tymcio, R.P., 2008. Mapping U.S. forest biomass using nationwide forest inventory data and moderate resolution information. Remote Sensing of Environment, Remote Sensing Data Assimilation Special Issue 112, 1658–1677. https://doi.org/10.1016/j.rse.2007.08.021

Brantley, S.T., Miniat, C.F., Bolstad, P.V., 2019. Rainfall partitioning varies across a forest age chronosequence in the southern Appalachian Mountains. Ecohydrology 12, e2081. https://doi.org/10.1002/eco.2081

Coogan, J., Dzwonkowski, B., Lehrter, J., 2019. Effects of Coastal Upwelling and Downwelling on Hydrographic Variability and Dissolved Oxygen in Mobile Bay. Journal of Geophysical Research: Oceans 124, 791–806. https://doi.org/10.1029/2018JC014592

Crockford, R.H., Richardson, D.P., 2000. Partitioning of rainfall into throughfall, stemflow and interception: effect of forest type, ground cover and climate. Hydrological Processes 14, 2903–2920. https://doi.org/10.1002/1099-1085(200011/12)14:16/17<2903::AID-HYP126>3.0.CO;2-6

Cunge, J.A., 1969. On The Subject Of A Flood Propagation Computation Method (Musklngum Method). Journal of Hydraulic Research 7, 205–230. https://doi.org/10.1080/00221686909500264

Deutsch, W.G., 2019. Alabama Rivers: A Celebration & Challenge. MindBridge Press.

Dickinson, R.E., 1987. Evapotranspiration in global climate models. Advances in Space Research 7, 17–26. https://doi.org/10.1016/0273-1177(87)90290-0

dos Santos, F.M., de Souza Pelinson, N., de Oliveira, R.P., Di Lollo, J.A., 2023. Using the SWAT model to identify erosion prone areas and to estimate soil loss and sediment transport in Mogi Guaçu River basin in Sao Paulo State, Brazil. CATENA 222, 106872. https://doi.org/10.1016/j.catena.2022.106872

Gorelick, N., Hancher, M., Dixon, M., Ilyushchenko, S., Thau, D., Moore, R., 2017. Google Earth Engine: Planetary-scale geospatial analysis for everyone. Remote Sensing of Environment, Big Remotely Sensed Data: tools, applications and experiences 202, 18–27. https://doi.org/10.1016/j.rse.2017.06.031

Grizzetti, B., Bouraoui, F., Granlund, K., Rekolainen, S., Bidoglio, G., 2003. Modelling diffuse emission and retention of nutrients in the Vantaanjoki watershed (Finland) using the SWAT model. Ecological Modelling 169, 25–38. https://doi.org/10.1016/S0304-3800(03)00198-4

Gu, Chunjie, Ma, J., Zhu, G., Yang, H., Zhang, K., Wang, Y., Gu, Chunli, 2018. Partitioning evapotranspiration using an optimized satellite-based ET model across biomes. Agricultural and Forest Meteorology 259, 355–363. https://doi.org/10.1016/j.agrformet.2018.05.023

Guo, T., Engel, B.A., Shao, G., Arnold, J.G., Srinivasan, R., Kiniry, J.R., 2018. Development and improvement of the simulation of woody bioenergy crops in the Soil and Water Assessment Tool (SWAT). Environmental Modelling & Software. https://doi.org/10.1016/j.envsoft.2018.08.030

Haas, H., Kalin, L., Srivastava, P., 2022a. Improved forest dynamics leads to better hydrological predictions in watershed modeling. Science of The Total Environment 821, 153180. https://doi.org/10.1016/j.scitotenv.2022.153180

Haas, H., Reaver, N.G.F., Karki, R., Kalin, L., Srivastava, P., Kaplan, D.A., Gonzalez-Benecke, C., 2022b. Improving the representation of forests in hydrological models. Science of The Total Environment 812, 151425. https://doi.org/10.1016/j.scitotenv.2021.151425

Haas, H., Reaver, N.G.F., Karki, R., Kalin, L., Srivastava, P., Kaplan, D.A., Gonzalez-Benecke, C., 2021. Improving the representation of forests in hydrological models. Science of The Total Environment 151425. https://doi.org/10.1016/j.scitotenv.2021.151425

Hadiwijaya, B., Isabelle, P.-E., Nadeau, D.F., Pepin, S., 2021. Observations of canopy storage capacity and wet canopy evaporation in a humid boreal forest. Hydrological Processes 35, e14021. https://doi.org/10.1002/hyp.14021

Isik, S., Haas, H., Kalin, L., Hantush, M.M., Nietch, C., 2023. Nutrient Removal Potential of Headwater Wetlands in Coastal Plains of Alabama, USA. Water 15, 2687. https://doi.org/10.3390/w15152687

J. McCarthy, E., W. Skaggs, R., Famum, P., 1991. EXPERIMENTAL DETERMINATION OF THE HYDROLOGIC COMPONENTS OF A DRAINED FOREST WATERSHED. Transactions of the ASAE 34, 2031–2039. https://doi.org/10.13031/2013.31833

Jiang, M., Peng, H., Liang, S., Wang, S., Kalin, L., Baltaci, E., Liu, Y., 2023. Impact of extreme rainfall on non-point source nitrogen loss in coastal basins of Laizhou Bay, China. Science of The Total Environment 881, 163427. https://doi.org/10.1016/j.scitotenv.2023.163427

Johnson, G.C., Kidd, R.E., Journey, C.A., Zappia, H., Atkins, J.B., 2002. Environmental setting and water-quality issues of the Mobile River Basin, Alabama, Georgia, Mississippi, and Tennessee (USGS Numbered Series No. 2002–4162), Environmental setting and water-quality issues of the Mobile River Basin, Alabama, Georgia, Mississippi, and Tennessee, Water-Resources Investigations Report. https://doi.org/10.3133/wri024162

Karakoyun, E., Kaya, N., 2022. Hydrological simulation and prediction of soil erosion using the SWAT model in a mountainous watershed: a case study of Murat River Basin, Turkey. Journal of Hydroinformatics 24, 1175–1193. https://doi.org/10.2166/hydro.2022.056

Karki, R., Qi, J., Gonzalez-Benecke, C.A., Zhang, X., Martin, T.A., Arnold, J.G., 2023. SWAT-3PG: Improving forest growth simulation with a process-based forest model in SWAT. Environmental Modelling & Software 164, 105705. https://doi.org/10.1016/j.envsoft.2023.105705

Kofroňová, J., Šípek, V., Hnilica, J., Vlček, L., Tesař, M., 2021. Canopy interception estimates in a Norway spruce forest and their importance for hydrological modelling. Hydrological Sciences Journal 66, 1233–1247. https://doi.org/10.1080/02626667.2021.1922691

Komatsu, H., Kume, T., 2020. Modeling of evapotranspiration changes with forest management practices: A genealogical review. Journal of Hydrology 585, 124835. https://doi.org/10.1016/j.jhydrol.2020.124835

Lai, G., Luo, J., Li, Q., Qiu, L., Pan, R., Zeng, X., Zhang, L., Yi, F., 2020. Modification and validation of the SWAT model based on multi-plant growth mode, a case study of the Meijiang River Basin, China. Journal of Hydrology 585, 124778. https://doi.org/10.1016/j.jhydrol.2020.124778

Lawrence, D.M., Thornton, P.E., Oleson, K.W., Bonan, G.B., 2007. The Partitioning of Evapotranspiration into Transpiration, Soil Evaporation, and Canopy Evaporation in a GCM: Impacts on Land–Atmosphere Interaction. Journal of Hydrometeorology 8, 862–880. https://doi.org/10.1175/JHM596.1

Leyton, L., Reynolds, E.R.C., Thompson, T., 1967. Rainfall Interception in Forest and Moorland, in: International Symposium on Forest Hydrology. Presented at the International Symposium on forest hydrology, Forest Hydrology, Pergamon, Oxford., pp. 163-178.

Li Zejun, Liu Pan, Feng Maoyuan, Cui Xueqing, He Ping, Wang Caijun, Zhang Jingwen, 2020. Evaluating the Effect of Transpiration in Hydrologic Model Simulation through Parameter Calibration. Journal of Hydrologic Engineering 25, 04020007. https://doi.org/10.1061/(ASCE)HE.1943-5584.0001895

Liang, K., Qi, J., Zhang, X., Deng, J., 2022. Replicating measured site-scale soil organic carbon dynamics in the U.S. Corn Belt using the SWAT-C model. Environmental Modelling & Software 158, 105553. https://doi.org/10.1016/j.envsoft.2022.105553

Luo, Z., Zhang, H., Pang, J., Yang, J., Li, M., 2023. Coupling of SWAT and EPIC Models to Investigate the Mutual Feedback Relationship between Vegetation and Soil Erosion, a Case Study in the Huangfuchuan Watershed, China. Forests 14, 844. https://doi.org/10.3390/f14040844

McLaughlin, D.L., Kaplan, D.A., Cohen, M.J., 2013. Managing Forests for Increased Regional Water Yield in the Southeastern U.S. Coastal Plain. JAWRA Journal of the American Water Resources Association 49, 953–965. https://doi.org/10.1111/jawr.12073

Miralles, D.G., De Jeu, R. a. M., Gash, J.H., Holmes, T.R.H., Dolman, A.J., 2011a. Magnitude and variability of land evaporation and its components at the global scale. Hydrology and Earth System Sciences 15, 967–981. https://doi.org/10.5194/hess-15-967-2011

Miralles, D.G., Gash, J.H., Holmes, T.R.H., de Jeu, R.A.M., Dolman, A.J., 2010. Global canopy interception from satellite observations. Journal of Geophysical Research: Atmospheres 115. https://doi.org/10.1029/2009JD013530

Miralles, D.G., Holmes, T.R.H., Jeu, R.A.M.D., Gash, J.H., Meesters, A.G.C.A., Dolman, A.J., 2011b. Global land-surface evaporation estimated from satellite-based observations. Hydrology and Earth System Sciences 15, 453–469. https://doi.org/10.5194/hess-15-453-2011

Monteith, J.L., 1965. Evaporation and environment. Symposia of the Society for Experimental Biology 19, 205–234.

Moriasi, D.N., Arnold, J.G., Liew, M.W.V., Bingner, R.L., Harmel, R.D., Veith, T.L., 2007. Model evaluation guidelines for systematic quantification of accuracy in watershed simulations.

Mu, Q., Zhao, M., Running, S.W., 2013. MODIS Global Terrestrial Evapotranspiration (ET) Product (NASE MOD16A2/A3). Algorithm Theoretical Basis Document, Collectio, 5, 600.

Muzylo, A., Llorens, P., Valente, F., Keizer, J.J., Domingo, F., Gash, J.H.C., 2009. A review of rainfall interception modelling. Journal of Hydrology 370, 191–206. https://doi.org/10.1016/j.jhydrol.2009.02.058

Nair, S.S., King, K.W., Witter, J.D., Sohngen, B.L., Fausey, N.R., 2011. Importance of Crop Yield in Calibrating Watershed Water Quality Simulation Tools1. JAWRA Journal of the American Water Resources Association 47, 1285–1297. https://doi.org/10.1111/j.1752-1688.2011.00570.x

Neitsch, S.L., Arnold, J.G., Kiniry, J.R., Williams, J.R., 2011. Soil and water assessment tool theoretical documentation: version 2009. Texas Water Resources Institute Technical Report No. 406. Texas Water Resources Institute, USA.

Nicholls, E.M., Carey, S.K., 2021. Evapotranspiration and energy partitioning across a forest-shrub vegetation gradient in a subarctic, alpine catchment. Journal of Hydrology 602, 126790. https://doi.org/10.1016/j.jhydrol.2021.126790

Noilhan, J., Planton, S., 1989. A Simple Parameterization of Land Surface Processes for Meteorological Models. Monthly Weather Review 117, 536–549. https://doi.org/10.1175/1520-0493(1989)117<0536:ASPOLS>2.0.CO;2

Oki, T., Kanae, S., 2006. Global Hydrological Cycles and World Water Resources. Science 313, 1068–1072. https://doi.org/10.1126/science.1128845

Oleson, K.W., Lawrence, D.M., Bonan, G.B., Drewniak, B., Huang, M., Levis, S., Li, F., Riley, W.J., Swenson, S.C., Thornton, P.E., Bozbiyik, A., Fisher, R., Heald, C.L., Kluzek, E., Lamarque, F., Lawrence, P.J., Leung, L.R., Muszala, S., Ricciuto, D.M., Sacks, W., Sun, Y., Tang, J., Yang, Z.-L., 2013. Technical Description of version 4.5 of the Community Land Model (CLM). NCAR Earth System Laboratory Climate and Global Dynamics Division, National Center for Atmospheric Research, Boulder, Colorado.

Parajuli, P.B., Jayakody, P., Ouyang, Y., 2018. Evaluation of Using Remote Sensing Evapotranspiration Data in SWAT. Water Resour Manage 32, 985–996. https://doi.org/10.1007/s11269-017-1850-z

Paul-Limoges, E., Wolf, S., Schneider, F.D., Longo, M., Moorcroft, P., Gharun, M., Damm, A., 2020. Partitioning evapotranspiration with concurrent eddy covariance measurements in a mixed forest. Agricultural and Forest Meteorology 280, 107786. https://doi.org/10.1016/j.agrformet.2019.107786

Rajib, A., Evenson, G.R., Golden, H.E., Lane, C.R., 2018a. Hydrologic model predictability improves with spatially explicit calibration using remotely sensed evapotranspiration and biophysical parameters. Journal of Hydrology 567, 668–683. https://doi.org/10.1016/j.jhydrol.2018.10.024

Rajib, A., Kim, I.L., Golden, H.E., Lane, C.R., Kumar, S.V., Yu, Z., Jeyalakshmi, S., 2020. Watershed Modeling with Remotely Sensed Big Data: MODIS Leaf Area Index Improves Hydrology and Water Quality Predictions. Remote Sensing 12, 2148. https://doi.org/10.3390/rs12132148

Rajib, A., Merwade, V., Yu, Z., 2018b. Rationale and Efficacy of Assimilating Remotely Sensed Potential Evapotranspiration for Reduced Uncertainty of Hydrologic Models. Water Resources Research 54, 4615–4637. https://doi.org/10.1029/2017WR021147

Rajib, M.A., Merwade, V., Yu, Z., 2016. Multi-objective calibration of a hydrologic model using spatially distributed remotely sensed/in-situ soil moisture. Journal of Hydrology 536, 192–207. https://doi.org/10.1016/j.jhydrol.2016.02.037

Richter, B.D., Baumgartner, J.V., Powell, J., Braun, D.P., 1996. A Method for Assessing Hydrologic Alteration within Ecosystems. Conservation Biology 10, 1163–1174. https://doi.org/10.1046/j.1523-1739.1996.10041163.x

Robinson, N.P., Allred, B.W., Smith, W.K., Jones, M.O., Moreno, A., Erickson, T.A., Naugle, D.E., Running, S.W., 2018. Terrestrial primary production for the conterminous United States derived from Landsat 30 m and MODIS 250 m. Remote Sensing in Ecology and Conservation 4, 264–280. https://doi.org/10.1002/rse2.74

Ruefenacht, B., Finco, M.V., Nelson, M.D., Czaplewski, R., Helmer, E.H., Blackard, J.A., Holden, G.R., Lister, A.J., Salajanu, D., Weyermann, D., Winterberger, K., 2008. Conterminous U.S. and Alaska Forest Type Mapping Using Forest Inventory and Analysis Data. photogramm eng remote sensing 74, 1379–1388. https://doi.org/10.14358/PERS.74.11.1379

Running, S., Mu, Q., Zhao, M., 2015. MOD17A2H MODIS/Terra Gross Primary Productivity 8-Day L4 Global 500m SIN Grid V006. https://doi.org/10.5067/MODIS/MOD17A2H.006

Running, S., Zhao, M., 2019. MOD17A3HGF MODIS/Terra Net Primary Production Gap-Filled Yearly L4 Global 500 m SIN Grid V006 [Data set]. NASA EOSDIS Land Processes Distributed Active Archive Center. https://doi.org/10.5067/MODIS/MOD17A3HGF.006

Rutter, A.J., 1975. The hydrological cycle in vegetation. In J. L. Monteith (Ed.), Vegetation and the atmosphere, Academic Press. Academic Press.

Rutter, A.J., Kershaw, K.A., Robins, P.C., Morton, A.J., 1971. A predictive model of rainfall interception in forests, 1. Derivation of the model from observations in a plantation of Corsican pine. Agricultural Meteorology 9, 367–384. https://doi.org/10.1016/0002-1571(71)90034-3

Spittlehouse, D.L., Black, T.A., 1981. A growing season water balance model applied to two Douglas fir stands. Water Resources Research 17, 1651–1656. https://doi.org/10.1029/WR017i006p01651

Stoy, P.C., El-Madany, T.S., Fisher, J.B., Gentine, P., Gerken, T., Good, S.P., Klosterhalfen, A., Liu, S., Miralles, D.G., Perez-Priego, O., Rigden, A.J., Skaggs, T.H., Wohlfahrt, G., Anderson, R.G., Coenders-Gerrits, A.M.J., Jung, M., Maes, W.H., Mammarella, I., Mauder, M., Migliavacca, M., Nelson, J.A., Poyatos, R., Reichstein, M., Scott, R.L., Wolf, S., 2019. Reviews and syntheses: Turning the challenges of partitioning ecosystem evaporation and transpiration into opportunities. Biogeosciences 16, 3747–3775. https://doi.org/10.5194/bg-16-3747-2019

Strauch, M., Volk, M., 2013. SWAT plant growth modification for improved modeling of perennial vegetation in the tropics. Ecological Modelling 269, 98–112. https://doi.org/10.1016/j.ecolmodel.2013.08.013

Sun, G., Hallema, D., Asbjornsen, H., 2017. Ecohydrological processes and ecosystem services in the Anthropocene: a review. Ecological Processes 6, 35. https://doi.org/10.1186/s13717-017-0104-6

Tang, G., Beckage, B., Smith, B., Miller, P.A., 2010. Estimating potential forest NPP, biomass and their climatic sensitivity in New England using a dynamic ecosystem model. Ecosphere 1, art18. https://doi.org/10.1890/ES10-00087.1

Tobin, K.J., Bennett, M.E., 2017. Constraining SWAT Calibration with Remotely Sensed Evapotranspiration Data. JAWRA Journal of the American Water Resources Association 53, 593–604. https://doi.org/10.1111/1752-1688.12516

Venkatesh, K., Preethi, K., Ramesh, H., 2020. Evaluating the effects of forest fire on water balance using fire susceptibility maps. Ecological Indicators 110, 105856. https://doi.org/10.1016/j.ecolind.2019.105856

Verseghy, D.L., McFarlane, N.A., Lazare, M., 1993. Class—A Canadian land surface scheme for GCMS, II. Vegetation model and coupled runs. International Journal of Climatology 13, 347–370. https://doi.org/10.1002/joc.3370130402

Wang, D., Wang, G., Anagnostou, E.N., 2007. Evaluation of canopy interception schemes in land surface models. Journal of Hydrology 347, 308–318. https://doi.org/10.1016/j.jhydrol.2007.09.041

Williams, J.J.R., 1975. Sediment-yield prediction with Universal Equation using runoff energy factor [WWW Document]. URL /paper/Sediment-yield-prediction-with-Universal-Equation-Williams/a9bc4612310f980c973575cbf86c63b77a01ace1 (accessed 7.18.20).
Williams, J.R., 1990. The erosion-productivity impact calculator (EPIC) model: a case history. Phil. Trans. R. Soc. Lond. B 329, 421–428. https://doi.org/10.1098/rstb.1990.0184
Yang, M., Zuo, R., Wang, L., Chen, X., 2018. A Simulation Study of Global Evapotranspiration Components Using the Community Land Model. Atmosphere 9, 178. https://doi.org/10.3390/atmos9050178
Yang, Q., Almendinger, J.E., Zhang, X., Huang, M., Chen, X., Leng, G., Zhou, Y., Zhao, K., Asrar, G.R., Srinivasan, R., Li, X., 2018. Enhancing SWAT simulation of forest ecosystems for water resource assessment: A case study in the St. Croix River basin. Ecological Engineering 120, 422–431. https://doi.org/10.1016/j.ecoleng.2018.06.020
Yang, Q., Zhang, X., 2016. Improving SWAT for simulating water and carbon fluxes of forest ecosystems. Science of The Total Environment 569–570, 1478–1488. https://doi.org/10.1016/j.scitotenv.2016.06.238
Yen, H., Bailey, R.T., Arabi, M., Ahmadi, M., White, M.J., Arnold, J.G., 2014. The Role of Interior Watershed Processes in Improving Parameter Estimation and Performance of Watershed Models. Journal of Environment Quality 43, 1601. https://doi.org/10.2134/jeq2013.03.0110
Yu, L., Zhou, S., Zhao, X., Gao, X., Jiang, K., Zhang, B., Cheng, L., Song, X., Siddique, K.H.M., 2022. Evapotranspiration Partitioning Based on Leaf and Ecosystem Water Use Efficiency. Water Resources Research 58, e2021WR030629. https://doi.org/10.1029/2021WR030629
Zhang, S., Hao, X., Zhao, Z., Zhang, J., Fan, X., Li, X., 2023. Natural Vegetation Succession Under Climate Change and the Combined Effects on Net Primary Productivity. Earth's Future 11, e2023EF003903. https://doi.org/10.1029/2023EF003903
Zhang, Y., Kong, D., Gan, R., Chiew, F.H.S., McVicar, T.R., Zhang, Q., Yang, Y., 2019. Coupled estimation of 500 m and 8-day resolution global evapotranspiration and gross primary production in 2002–2017. Remote Sensing of Environment 222, 165–182. https://doi.org/10.1016/j.rse.2018.12.031
Zhang, Y., Peña-Arancibia, J.L., McVicar, T.R., Chiew, F.H.S., Vaze, J., Liu, C., Lu, X., Zheng, H., Wang, Y., Liu, Y.Y., Miralles, D.G., Pan, M., 2016. Multi-decadal trends in global terrestrial evapotranspiration and its components. Sci Rep 6, 19124. https://doi.org/10.1038/srep19124
Zore, A., Bezak, N., Šraj, M., 2022. The influence of rainfall interception on the erosive power of raindrops under the birch tree. Journal of Hydrology 613, 128478. https://doi.org/10.1016/j.jhydrol.2022.128478